

(Pentamethylcyclopentadienyl)molybdenum Bromides and Iodides

Jahani U. Desai,[†] John C. Gordon,[†] Heinz-Bernhard Kraatz,[†] Vincent T. Lee,[†]
Beth E. Owens-Waltermire,[‡] Rinaldo Poli,^{*,†,§} Arnold L. Rheingold,[‡] and Corbet B. White[‡]

Department of Chemistry and Biochemistry, University of Maryland, College Park, Maryland 20742,
and Department of Chemistry, University of Delaware, Newark, Delaware 19716

Received September 1, 1993*

Contrary to the (pentamethylcyclopentadienyl)trichloromolybdenum(IV) system, for which the molecular $[\text{Cp}^*\text{MoCl}_2(\mu\text{-Cl})]_2$ complex is the only form observed (Abugideiri, F.; Brewer, G. A.; Desai, J. U.; Gordon, J. C.; Poli, R. *Inorg. Chem.*, preceding paper in this issue), the corresponding chemistry of the heavier halide systems is much more complex. Three compounds or mixtures of compounds that correspond to the overall stoichiometry “ Cp^*MoX_3 ” ($X = \text{Br}, \text{I}$) can exist in the solid state and/or in solution [$\mathbf{A} = \text{Cp}^*_2\text{Mo}_2\text{X}_4(\mu\text{-X})_2$; $\mathbf{B} = \{[\text{Cp}^*_2\text{Mo}_2(\mu\text{-X})_4]^+[\text{Cp}^*\text{MoX}_4]^- + \text{Cp}^*\text{MoX}_4\}$; $\mathbf{C} = [\text{Cp}^*_2\text{Mo}_2(\mu\text{-X})_4]^+(\text{X}^-)_{0.5}(\text{X}_3^-)_{0.5}$], and various combinations of them can be obtained depending on the halide nature, synthetic method and reaction conditions. Thermal decarbonylation of $\text{Cp}^*\text{MoX}_3(\text{CO})_2$ in refluxing toluene affords \mathbf{C} ($X = \text{Br}, \text{I}$) whereas the same treatment in dichloromethane affords \mathbf{A} ($X = \text{I}$) or an equilibrium mixture of \mathbf{A} and \mathbf{B} for $X = \text{Br}$. The equilibrium mixture of \mathbf{A} and \mathbf{B} for the bromide system is also obtained from dissolution of \mathbf{C} in CH_2Cl_2 , and from the reactions of $\text{Cp}^*_2\text{Mo}_2\text{Br}_4$ with Br_2 , Cp^*MoBr_4 with $\text{Cp}^*_2\text{Mo}_2\text{Br}_4$ (2:1 molar ratio), and $\text{Cp}^*_2\text{Mo}_2\text{Cl}_4$ with HBr, all carried out in dichloromethane solvent. From the reaction of $\text{Cp}^*_2\text{Mo}_2\text{Br}_4$ with Br_2 in benzene as solvent, the salt $[\text{Cp}^*_2\text{Mo}_2\text{Br}_4]^+(\text{Br}^-)_x(\text{Br}_3^-)_{1-x}$ with $x \approx 0.2$ has been obtained. For $X = \text{I}$, on the other hand, \mathbf{A} transforms into \mathbf{C} in refluxing toluene and the latter is stable in CH_2Cl_2 . Addition of I_2 to \mathbf{A} or \mathbf{C} ($X = \text{I}$) affords $[\text{Cp}^*_2\text{Mo}_2\text{I}_4]^+\text{I}_3^-$. Treatment of $\text{Cp}^*_2\text{Mo}_2\text{Cl}_4$ with HI affords only a mixed valence product of incomplete halide exchange, $[\text{Cp}^*_2\text{Mo}_2\text{I}_x\text{Cl}_{4-x}]^+\text{I}_3^-$. The molecular trihalide dimers (\mathbf{A} , $X = \text{Br}, \text{I}$) react with CO, PMe_3 , and X^- to afford the addition compounds $\text{Cp}^*\text{MoX}_3(\text{CO})_2$, $\text{Cp}^*\text{MoX}_3(\text{PMe}_3)$ (only $X = \text{Br}$), and $[\text{Cp}^*\text{MoX}_4]^-$. The latter ion shows a reversible one electron oxidation to the neutral Cp^*MoX_4 for $X = \text{Br}$, whereas for $X = \text{I}$ oxidation occurs preferentially at the I^- ligand, indicating the nonexistence of the Mo(V) compound Cp^*MoI_4 . System \mathbf{C} ($X = \text{I}$) does not add Lewis bases, whereas systems \mathbf{B} and \mathbf{C} with $X = \text{Br}$ do so only slowly in CH_2Cl_2 via preequilibration with \mathbf{A} . $\text{Cp}^*_2\text{Mo}_2\text{X}_4$ ($X = \text{Br}, \text{I}$) have been obtained by reduction of Cp^*MoBr_4 with Na/Hg in toluene or by reduction of $[\text{Cp}^*_2\text{Mo}_2\text{I}_4]\text{I}_3$ with PMe_3 , respectively. They exhibit two electrochemically reversible one-electron oxidations. Chemical oxidation with Ag^+ or NO^+ (only $X = \text{Br}$) in CH_2Cl_2 allows the isolation of $[\text{Cp}^*_2\text{Mo}_2\text{Br}_4]^+\text{BF}_4^-$ and $[\text{Cp}^*_2\text{Mo}_2\text{I}_4]^+\text{PF}_6^-$. Oxidation of $\text{Cp}^*_2\text{Mo}_2\text{Br}_4$ with Cp^*MoBr_4 affords stable solutions of $[\text{Cp}^*_2\text{Mo}_2\text{Br}_4]^+[\text{Cp}^*\text{MoBr}_4]^-$, which turn into an equilibrium mixture of \mathbf{A} and \mathbf{B} only after addition of an additional equivalent of Cp^*MoBr_4 . Crystal structures are reported for the following compounds: $\text{Cp}^*_2\text{Mo}_2\text{Br}_4$, $\text{Cp}^*_2\text{Mo}_2\text{Br}_6$ (two polymorphs), $\text{Cp}^*_2\text{Mo}_2\text{Br}_6\cdot\text{C}_6\text{H}_6$, $[\text{Cp}^*_2\text{Mo}_2\text{Br}_4]^{-2}\cdot\text{Cp}^*\text{MoBr}_4\cdot 2\text{C}_7\text{H}_{16}$, $[\text{Cp}^*_2\text{Mo}_2\text{I}_4]^+\text{I}_3^-$, $[\text{Cp}^*_2\text{Mo}_2\text{I}_2\text{Cl}_2]^+\text{I}_3^-$, and $[\text{NMe}_3\text{Ph}]^+[\text{Cp}^*\text{MoI}_4]$.

Introduction

We have been interested for some time in the development of preparative methods to monocyclopentadienylmolybdenum halide complexes, which are useful organometallic synthons.^{1–9} We have been successful in developing several synthetic strategies to the previously unknown Mo(IV) system CpMoCl_3 .⁸ More recent

extension of our work to the pentamethylcyclopentadienyl (Cp^*) system⁹ has allowed the preparation of soluble compounds suitable for structural, spectroscopic and mechanistic investigations. We have learned that the electrochemical properties of the mono-nuclear $[\text{Cp}^*\text{MoCl}_4]^{n-}$ ($n = 0, 1$) and dinuclear $[\text{Cp}^*_2\text{Mo}_2\text{Cl}_4]^{n+}$ ($n = 0, 1, 2$) systems play a fundamental role in this chemistry. Oxidation of $\text{Cp}^*_2\text{Mo}_2\text{Cl}_4$ by either PhICl_2 or Cp^*MoCl_4 produces the corresponding monocation, whereas reduction of Cp^*MoCl_4 affords the corresponding monoanion. A rapid chloride transfer reaction to the reactive $[\text{Cp}^*_2\text{Mo}_2\text{Cl}_4]^+$ ion then occurs to generate an observed $\text{Cp}^*_2\text{Mo}_2\text{Cl}_5$ intermediate, followed by further oxidation and chloride transfer with the ultimate formation of $\text{Cp}^*_2\text{Mo}_2\text{Cl}_6$ which has been structurally characterized as an antiferromagnetically coupled bis-halide-bridged dimer with no direct metal–metal bonding interaction.

In an attempt to extend the above studies to the analogous bromide and iodide systems, we have discovered a much more complex chemical behavior, which is mainly due, as will be shown in this contribution, to the greater stability of the $[\text{Cp}^*_2\text{Mo}_2\text{X}_4]^+$ ($X = \text{Br}, \text{I}$) ions with respect to the corresponding chloro complex and to the greater reducing power of the Br^- and I^- ions with respect to the Cl^- ion. There are only limited studies aimed at showing how the thermodynamic and redox stability for a given cyclopentadienylmetal halide system varies as the nature of the halide ligands is changed from chloride to bromide to iodide. It has been shown that the reduction potential of CpVBr_3 is ca. 50

* University of Maryland.

† University of Delaware.

‡ Presidential Young Investigator 1990–1995; Alfred P. Sloan Research Fellow 1992–1994.

* Abstract published in *Advance ACS Abstracts*, July 1, 1994.

- (1) Poli, R. *Chem. Rev.* 1991, 91, 509.
- (2) (a) Grebenik, P. D.; Green, M. L. H.; Izquierdo, A.; Mtetwa, V. S. B.; Prout, K. *J. Chem. Soc., Dalton Trans.* 1987, 9. (b) Green, M. L. H.; Hubert, J. D.; Mountford, P. J. *J. Chem. Soc., Dalton Trans.* 1990, 3793. (c) Cousins, M.; Green, M. L. H. *J. Chem. Soc. 1964*, 1567. (d) Cousins, M.; Green, M. L. H. *J. Chem. Soc. A 1969*, 16.
- (3) (a) Murray, R. C.; Blum, L.; Liu, A. H.; Schrock, R. R. *Organometallics* 1985, 4, 953. (b) Schrock, R. R.; Kolodziej, R. M.; Liu, A. H.; Davis, W. M.; Vale, M. G. *J. Am. Chem. Soc.* 1990, 112, 4338.
- (4) (a) Baker, R. T.; Calabrese, J. C.; Harlow, R. L.; Williams, I. D. *Organometallics* 1993, 12, 830. (b) Umakoshi, K.; Isobe, K. *J. Organomet. Chem.* 1990, 395, 47. (c) Rau, M. S.; Kretz, C. M.; Geoffroy, G. L.; Rheingold, A. L. *Organometallics* 1993, 12, 3447.
- (5) Krueger, S. T.; Owens, B. E.; Poli, R. *Inorg. Chem.* 1990, 29, 2001.
- (6) Poli, R.; Rheingold, A. L. *J. Chem. Soc., Chem. Commun.* 1990, 552.
- (7) Linck, R. G.; Owens, B. E.; Poli, R. *Gazz. Chim. Ital.* 1991, 121, 163.
- (8) (a) Poli, R.; Kelland, M. A. *J. Organomet. Chem.* 1991, 419, 127. (b) Gordon, J. C.; Lee, V.; Poli, R. *Inorg. Chem.* 1993, 32, 4460.
- (9) Abugideiri, F.; Brewer, G. A.; Desai, J. U.; Gordon, J. C.; Poli, R. *Inorg. Chem.*, preceding paper in this issue.

mV more positive than that of CpVCl_3 , indicating that higher oxidation state systems are more oxidizing when containing the heavier halogen.¹⁰ Since the heavier halide ions are more easily oxidized, oxidation of the halide ligands sometimes prevails over oxidation of the metal to generate salts of lower oxidation state metals with oxidized, polyhalide anions. This behavior is quite typical for the iodide compounds. For instance, although CpVI_3 contains V(IV) and iodide ligands in the solid state,¹ $^1\text{H-NMR}$ and cyclic voltammetric studies are in better agreement with a mixture of polyiodide systems of lower-valent vanadium in solution.¹⁰ Analogously, Cp^*CrI_3 has been shown to consist of a Cr(III) complex with a mixture of iodide and triiodide ligands rather than a molecular compound of Cr(IV).¹¹ In the present study, we also investigate the limits of stability of high oxidation state Cp^*Mo compounds with the heavier halides Br and I. Parts of this work have previously been communicated.^{12,13}

Experimental Section

General Data. Unless otherwise stated, all operations were carried out under an atmosphere of dinitrogen with standard Schlenk-line and glovebox techniques. Solvents were purified by conventional methods and distilled under dinitrogen prior to use. FT-IR spectra were recorded on a Perkin-Elmer 1800 spectrophotometer with 0.1-mm KBr liquid-sample cells (solutions) or KBr discs (Nujol mulls). NMR spectra were obtained with Bruker WP200 and AF200 spectrometers; the peak positions are reported upfield of TMS as calculated from the residual solvent peaks (^1H) or external 85% H_3PO_4 (^{31}P). For each $^{31}\text{P-NMR}$ spectrum, a sealed capillary containing H_3PO_4 and immersed in the same NMR solvent that had been used for the measurement was used as a reference. EPR spectra were recorded on a Bruker ER200 spectrometer equipped with an X-band microwave generator. Cyclic voltammograms were recorded with an EG&G 362 potentiostat connected to a Macintosh computer through MacLab hardware/software; the electrochemical cell was a locally modified Schlenk tube with a Pt counterelectrode sealed through uranium glass/Pyrex glass seals. All measurements were carried out with $n\text{-Bu}_4\text{NPF}_6$ (ca. 0.1 M) as the supporting electrolyte. The cell was fitted with a Ag/AgCl reference electrode and a Pt working electrode and all potentials are reported vs the $\text{Cp}_2\text{Fe}/\text{Cp}_2\text{Fe}^+$ couple which was introduced into the cell at the end of each measurement. Magnetic susceptibility measurements were carried out at room temperature with a commercial Johnson Matthey balance and were corrected for the diamagnetism of the ligands by using Pascal's constants before conversion to magnetic moments. The elemental analyses were by M-H-W Laboratories, Phoenix, AZ, or Galbraith Laboratories, Inc., Knoxville, TN. Cp^*MoBr_4 was prepared from $[\text{Cp}^*\text{Mo}(\text{CO})_3]_2$ and 2 equiv of PBr_3 in CH_2Cl_2 (yield 88% on a 8 g scale). Anal. Calcd for $\text{C}_{10}\text{H}_{15}\text{Br}_4\text{Mo}$: C, 21.81; H, 2.74; Br, 58.02. Found: C, 21.8; H, 2.8; Br, 59.9. The preparation of the analogous ($\eta\text{-C}_5\text{H}_4\text{Me}$) MoBr_4 by the same method is described in the literature.^{2b} $\text{Cp}^*\text{Mo}_2\text{Cl}_4$ ⁹ and $\text{Cp}^*\text{MoI}_3(\text{CO})_2$ ^{13,14} were prepared according to the known procedures. Gaseous HBr and HI (Matheson, $\text{NMe}_3\text{Ph}^+\text{I}^-$ and $\text{Bu}_4\text{N}^+\text{I}^-$ (Eastman Kodak) and $\text{Bu}_4\text{N}^+\text{Br}^-$ (Aldrich) were used without further purification.

Reduction of Cp^*MoBr_4 with Amalgamated Sodium. Preparation of $\text{Cp}^*\text{Mo}_2\text{Br}_4$. Cp^*MoBr_4 (3.427 g, 6.22 mmol) was placed in a Schlenk tube in which sodium amalgam (311 mg of Na, 13.5 mmol in 31 g of Hg) had been previously prepared. Toluene (40 mL) was subsequently added. The dark suspension was allowed to stir at room temperature overnight, during which time the solution had developed a tan brown color. The mixture was filtered and the precipitate washed with toluene until the filtered solution was colorless (4 \times 20 mL). The combined filtrates were concentrated under reduced pressure and then cooled to -20 °C to yield 2.183 g (89.9%) of product. Anal. Calcd for $\text{C}_{10}\text{H}_{15}\text{Br}_2\text{Mo}$: C, 30.72; H, 3.87. Found: C, 30.6; H, 3.9. $^1\text{H-NMR}$ (δ , CDCl_3): 1.93. Cyclic voltammogram (CH_2Cl_2): -0.30 V (reversible $\text{Cp}^*\text{Mo}_2\text{Br}_4/[Cp^*\text{Mo}_2\text{Br}_4]^+$,

$\Delta E_p = 107 \text{ mV}$), +0.73 V (reversible $[\text{Cp}^*\text{Mo}_2\text{Br}_4]^+/\text{Cp}^*\text{Mo}_2\text{Br}_4\text{Cl}^{2+}$, $\Delta E_p = 98 \text{ mV}$); the $\text{Cp}_2\text{Fe}/\text{Cp}_2\text{Fe}^+$ couple had $\Delta E_p = 121 \text{ mV}$. The reversibility and the potential of these two waves did not change when free Br^- was added to the solution. A crystal of this compound for the X-ray analysis was obtained by recrystallization from hot heptane.

The same product was obtained when the reduction was carried out with 1 equiv of sodium, in an attempt to produce a Mo(IV) product. Cp^*MoBr_4 (1.821 g, 3.31 mmol) and amalgamated sodium (74 mg, 3.22 mmol in ca. 10 g Hg) were suspended in 20 mL of toluene. After overnight stirring at room temperature, the yellow-brown suspension was evaporated to dryness, the residue was extracted with CH_2Cl_2 (ca. 50 mL), and the resulting solution was filtered and evaporated to dryness. A total of 1.127 g of yellow-brown solid was recovered. $^1\text{H-NMR}$ and analytical data (found: C, 31.25; H, 4.15) for this material were in accord with the Mo(III) product prepared as described above. On the basis of the amount of limiting reagent (Na), the yield was 89.5%.

Preparation of $[\text{Cp}^*\text{Mo}_2\text{Br}_4]\text{BF}_4^-$. (a) **From $\text{Cp}^*\text{Mo}_2\text{Br}_4$ and AgBF_4 .** $\text{Cp}^*\text{Mo}_2\text{Br}_4$ (114 mg, 0.146 mmol) was introduced into a Schlenk tube and dissolved in CH_2Cl_2 (20 mL). To the resulting light yellow solution was added AgBF_4 (28 mg, 0.15 mmol). The color changed immediately to brown and then to purple and finally to red after 10 min while a gray precipitate formed. The solution was filtered, reduced in volume to ca. 2 mL by evaporation at reduced pressure, and then heptane (20 mL) was added. The resulting red precipitate was washed with heptane (2 \times 20 mL) and then with pentane (2 \times 10 mL) and finally dried under vacuum. Yield: 107 mg (84%). Anal. Calcd for $\text{C}_{20}\text{H}_{30}\text{Br}_4\text{F}_4\text{Mo}_2$: C, 27.65; H, 3.84. Found: C, 27.81; H, 3.81. $^1\text{H-NMR}$ (δ , CDCl_3): 4.3 (broad, $w_{1/2} = 120 \text{ Hz}$).

(b) **From $\text{Cp}^*\text{Mo}_2\text{Br}_4$ and NOBF_4 .** $\text{Cp}^*\text{Mo}_2\text{Br}_4$ (187 mg, 0.239 mmol) was dissolved in CH_2Cl_2 (20 mL) to give a brown solution. To the stirring solution was added solid NOBF_4 (28 mg, 0.24 mmol). The solution slowly changed color to orange-brown. Stirring was continued for 1 h. The clear orange-brown solution was filtered and reduced in volume to 5 mL. A red precipitate was obtained by adding pentane (20 mL). The precipitate was washed with pentane (2 \times 10 mL) and then dried under vacuum. Yield: 170 mg (82%). The NMR properties are identical with those described above for the product of oxidation with AgBF_4 .

Reaction between $\text{Cp}^*\text{Mo}_2\text{Br}_4$ and Br_2 . (a) **In Benzene.** Preparation of $[\text{Cp}^*\text{Mo}_2\text{Br}_4]^+(\text{Br}^-)_x(\text{Br}_3^-)_{1-x}$ and Crystallization of $\{[\text{Cp}^*\text{Mo}_2\text{Br}_4]^+(\text{Br}^-)_x(\text{Br}_3^-)_{1-x}\}_2\text{Cp}^*\text{MoBr}_4$. $\text{Cp}^*\text{Mo}_2\text{Br}_4$ (538 mg, 0.69 mmol) was dissolved in benzene (10 mL). A solution of Br_2 (35 μL , 0.69 mmol) in benzene (5 mL) was added, causing the instantaneous formation of a red precipitate. The product was collected by filtration, washed with heptane, and dried under vacuum. Yield: 381 mg. $^1\text{H-NMR}$ (δ , CDCl_3): 4.3 (br, $w_{1/2} = 120 \text{ Hz}$). The NMR resonance has identical position and linewidth with the resonance observed for the $[\text{Cp}^*\text{Mo}_2\text{Br}_4]^+$ cation in the BF_4^- salt (see previous section); the only other resonance observed in the $^1\text{H-NMR}$ spectrum was that of the solvent. The elemental analysis of this crude material was consistent with the approximate stoichiometry $\text{Cp}^*\text{MoBr}_{3.3}$ (Anal. Calcd for $\text{C}_{10}\text{H}_{15}\text{Br}_{3.3}\text{Mo}$: C, 24.27; H, 3.06. Found: C, 24.2; H, 2.3), indicating a composition $[\text{Cp}^*\text{Mo}_2\text{Br}_4]^+(\text{Br}^-)_x(\text{Br}_3^-)_{1-x}$ with $x = 0.2$ and a 72% yield with respect to Br_2 . The cyclic voltammogram of this compound in CH_2Cl_2 is discussed in the Results section.

From the recrystallization of this crude material from CH_2Cl_2 /heptane, dark red platelike crystals were obtained. One of these crystals was investigated by X-ray diffraction and found to have the composition $[\text{Cp}^*\text{Mo}_2\text{Br}_4]_2[\text{Cp}^*\text{MoBr}_4]_3\text{C}_2\text{H}_{16}$. The $^1\text{H-NMR}$ of these crystals in CDCl_3 exhibited two broad peaks at δ 4.2 ($w_{1/2} = 80 \text{ Hz}$) and -19.5 ($w_{1/2} = 270 \text{ Hz}$). The mother liquor of the crystals also showed, in addition to the same resonances of the crystals, a minor sharp singlet at δ 2.06 and a broad resonance at δ -5.7 ($w_{1/2} = 33 \text{ Hz}$) due to $\text{Cp}^*\text{Mo}_2\text{Br}_6$ (vide infra).

(b) **In Dichloromethane. Crystallization of $\text{Cp}^*\text{Mo}_2\text{Br}_6\text{C}_6\text{H}_6$.** $\text{Cp}^*\text{Mo}_2\text{Br}_4$ (569 mg, 0.73 mmol) was dissolved in CH_2Cl_2 (40 mL) and to the resulting solution was added dropwise a solution of Br_2 (35 mL, 0.68 mmol) in 10 mL of CH_2Cl_2 . A color change from yellow-brown to dark brown was observed during the addition. The solution was evaporated to dryness leaving 582 mg of a crude residue whose $^1\text{H-NMR}$ spectrum in CDCl_3 showed resonances at δ 4.0 ($w_{1/2} = 60 \text{ Hz}$) and -19.0 ($w_{1/2} = 230 \text{ Hz}$), consistent with the formation of $[\text{Cp}^*\text{Mo}_2\text{Br}_4][\text{Cp}^*\text{MoBr}_4]$ (see Results). Recrystallization of this material from 1,1,2-C₂H₃Cl₃/benzene gave a mixture of red crystals and powder whose $^1\text{H-NMR}$ spectrum in CDCl_3 showed, in addition to the resonances of the crude material, new resonances at δ 2.05 (sharp) and -5.7 (broad). An X-ray analysis on one of the crystals showed this to be $\text{Cp}^*\text{Mo}_2\text{Br}_6\text{C}_6\text{H}_6$.

- (10) Morse, D. B.; Rauchfuss, T. B.; Wilson, S. R. *Inorg. Chem.* 1991, 30, 775.
- (11) Morse, D. B.; Rauchfuss, T. B.; Wilson, S. R. *J. Am. Chem. Soc.* 1990, 112, 1860.
- (12) Desai, J. U.; Gordon, J. C.; Kraatz, H.-B.; Owens-Waltermire, B. E.; Poli, R.; Rheingold, A. L. *Angew. Chem., Int. Ed. Engl.* 1993, 32, 1486.
- (13) Poli, R.; Gordon, J. C.; Desai, J. U.; Rheingold, A. L. *J. Chem. Soc., Chem. Commun.* 1991, 1518.
- (14) Adams, H.; Bailey, N. A.; Bentley, G. W.; Hough, G.; Winter, M. J.; Woodward, S. J. *Chem. Soc., Dalton Trans.* 1991, 749.

Synthesis of $\text{Cp}^*\text{MoBr}_3(\text{CO})_2$. In a Schlenk tube equipped with a magnetic stirrer bar and a pressure-equalized dropping funnel was suspended $[\text{Cp}^*\text{Mo}(\text{CO})_3]_2$ (0.51 g, 0.81 mmol) in CH_2Cl_2 (4 mL). From the funnel, 0.13 mL of Br_2 (2.52 mmol) in heptane (26 mL) was added dropwise to the stirred suspension. Evolution of gas bubbles was observed, as was the darkening of the solution to a deep red color. After stirring for 2 h, the orange solid that had formed was collected by filtration, washed with heptane (20 mL), and dried under vacuum. Yield: 0.80 g (94%). IR ($\nu_{\text{CO}}/\text{cm}^{-1}$, CH_2Cl_2): 2076 s, 2041 s. $^1\text{H-NMR}$ (δ , CD_2Cl_2): 2.19 (s). Anal. Calcd for $\text{C}_{12}\text{H}_{15}\text{MoO}_2\text{Br}_3$: C, 27.35; H, 2.87. Found: 27.0; H, 2.9.

Thermal Decarbonylation of $\text{Cp}^*\text{MoBr}_3(\text{CO})_2$. (a) In Toluene. Preparation of $[\text{Cp}^*\text{Mo}_2\text{Br}_4]^+(\text{Br}^-)_{0.5}(\text{Br}_3)^{-0.5}$. $\text{Cp}^*\text{MoBr}_3(\text{CO})_2$ (0.75 g, 1.42 mmol) was placed in a Schlenk tube equipped with a stirrer bar and a reflux condenser. Toluene (20 mL) was added and the suspension was refluxed for 5 days resulting in the formation of a brown solution and a brown microcrystalline precipitate. The product was collected by filtration, washed with heptane (15 mL), and dried under vacuum. Yield: 299 mg. IR spectroscopy (Nujol mull) indicated that this solid contained no residual CO. This compound analyzed correctly for Cp^*MoBr_3 . Anal. Calcd for $\text{C}_{10}\text{H}_{15}\text{Br}_3\text{Mo}$: C, 25.51; H, 3.21. Found: C, 25.3; H, 3.4. $^1\text{H-NMR}$ (δ , CDCl_3): 4.6 (br, $w_{1/2} = 70$ Hz). This resonance is attributed to the $[\text{Cp}^*\text{Mo}_2\text{Br}_4]^+$ cation. No other resonances attributable to Cp^* protons were observed in spectrum within the $\delta +70$ to -70 range. When the same reaction was carried out with only overnight reflux in toluene, however, the isolated solid (447 mg from 0.86 mmol of $\text{Cp}^*\text{MoBr}_3(\text{CO})_2$) had a more complex NMR spectrum, showing a broad peak at δ 3.7, a minor sharp singlet at δ 2.05, and a broad peak at δ -5.6.

(b) In Dichloromethane. $\text{Cp}^*\text{MoBr}_3(\text{CO})_2$ was made in situ as described above from $[\text{Cp}^*\text{Mo}(\text{CO})_3]_2$ (1.007 g, 1.60 mmol) and Br_2 (250 mL, 4.85 mmol) in 20 mL of CH_2Cl_2 . Once this step was complete as verified by IR spectroscopy, the mixture was refluxed for 2 days, producing a dark brown solution which had no residual CO (by IR spectroscopy). The solution was reduced in volume, and heptane (30 mL) was added. The resulting dark brown precipitate was collected by filtration and dried under vacuum. Yield: 936 mg. Anal. Found: C, 24.1; H, 3.4. The $^1\text{H-NMR}$ of this material (CDCl_3) was complex, with resonances at δ 4.5 (br, $w_{1/2} = 80$ Hz), 2.06 (sharp s, $w_{1/2}$ ca. 1 Hz), -5.7 (br, $w_{1/2} = 30$ Hz) and -19.5 (br, $w_{1/2} = 200$ Hz). The assignment of these resonances is given in the Results section.

Reaction between $\text{Cp}^*\text{Mo}_2\text{Cl}_4$ and HBr. Crystallization of $\text{Cp}^*\text{Mo}_2\text{Br}_6$. $\text{Cp}^*\text{Mo}_2\text{Cl}_4$ (566 mg, 0.94 mmol) was dissolved in CH_2Cl_2 (20 mL) and a constant stream of gaseous HBr was bubbled through the solution for ca. 1 h. During this time the originally light brown solution became dark red-brown and a small amount of dark precipitate formed. The solution was evaporated to dryness to obtain 340 mg of black microcrystalline crude product. The $^1\text{H-NMR}$ spectrum (CDCl_3) was complex, the most prominent features being broad resonances at δ 4.0 ($w_{1/2} = 200$ Hz) and -19.5 ($w_{1/2} = 275$ Hz) in a 2:1 ratio, consistent with the formation of $[\text{Cp}^*\text{Mo}_2\text{Br}_4]^+[\text{Cp}^*\text{MoBr}_4]^-$ (see Results).

The preparation and NMR properties of this product were reproducible. However, recrystallization of the crude product afforded, on different occasions, either dark red rod-like crystals which had an identical $^1\text{H-NMR}$ spectrum with that of the crude material or red crystals with a different $^1\text{H-NMR}$ spectrum, both repeatedly and under identical conditions (diffusion of a heptane layer into a CH_2Cl_2 solution at room temperature). The former crystals lost solvent of crystallization very easily and they could not be used for an X-ray analysis (the presence of CH_2Cl_2 in this material was confirmed by $^1\text{H-NMR}$). The latter crystals were shown by X-ray analysis to consist of $\text{Cp}^*\text{Mo}_2\text{Br}_6$ (two polymorphs). Anal. Calcd for $\text{C}_{10}\text{H}_{15}\text{Br}_3\text{Mo}$: C, 25.51; H, 3.16. Found: C, 25.4; H, 3.5. $^1\text{H-NMR}$ (δ , CDCl_3): -5.7 (br, $w_{1/2} = 30$ Hz). $^1\text{H-NMR}$ (δ , CD_2Cl_2): -6.0 (br, $w_{1/2} = 25$ Hz). A minor sharp singlet at δ 2.06 was also observed in these spectra, its relative intensity with respect to that of the major product varying from sample to sample but being typically within 10% of the total integrated intensity.

Reaction between Cp^*MoBr_4 and $\text{Cp}^*\text{Mo}_2\text{Br}_4$. (a) In a 1:1 Ratio. $\text{Cp}^*\text{Mo}_2\text{Br}_4$ (17 mg, 0.021 mmol) and Cp^*MoBr_4 (11 mg, 0.020 mmol) were introduced into a Schlenk tube and dissolved in 1 mL of CDCl_3 . The resulting orange-brown solution was transferred into a thin-walled 5-mm NMR tube and immediately investigated by $^1\text{H-NMR}$: 4.1 (br, $w_{1/2} = 85$ Hz, 30 H), -19.5 (br, $w_{1/2} = 140$ Hz, 15 H). This spectrum did not further change over several hours at room temperature.

(b) In a 2:1 Ratio. To a Schlenk tube, $\text{Cp}^*\text{Mo}_2\text{Br}_4$ (17 mg, 0.021 mmol) and Cp^*MoBr_4 (23 mg, 0.042 mmol) were added and then dissolved

in 1 mL of CDCl_3 . The orange-brown solution was immediately transferred into a thin-walled 5-mm NMR tube and sealed for spectroscopic monitoring purposes. $^1\text{H-NMR}$: initial, δ 4.1 and -19.5; final, δ 4.1 (4.7 H), 2.06 (minor), -5.7 (1 H), -19.5 (4.9 H). The spectrum did not further change after ca. 7 h at room temperature.

Addition of Br^- to the Mixture of Approximate Composition " Cp^*MoBr_3 ". (a) Qualitative NMR Monitoring. A sample of " Cp^*MoBr_3 " obtained from the decarbonylation of $\text{Cp}^*\text{MoBr}_3(\text{CO})_2$ in dichloromethane (e.g. containing $\text{Cp}^*\text{Mo}_2\text{Br}_6$, $[\text{Cp}^*\text{Mo}_2\text{Br}_4]$, $[\text{Cp}^*\text{MoBr}_4]$ and Cp^*MoBr_3 , see Results section) was dissolved in CDCl_3 and treated with an excess of $n\text{-Bu}_4\text{NBr}$. $^1\text{H-NMR}$ monitoring showed that the resonance due to $\text{Cp}^*\text{Mo}_2\text{Br}_6$ (δ -5.7) disappeared immediately in favor of the increase of the resonance at δ -19.5. Subsequently, the resonance at δ 4.5 slowly decreased while the resonance at δ -19.5 continued to increase. After ca. 2 days at room temperature, the resonance at δ -19.5 was the only Cp^* resonance remaining in the spectrum.

(b) Preparation of $[\text{n-Bu}_4\text{N}]^+[\text{Cp}^*\text{MoBr}_4]$. A sample of " Cp^*MoBr_3 " obtained from the decarbonylation of $\text{Cp}^*\text{MoBr}_3(\text{CO})_2$ in dichloromethane (436 mg, 0.926 mmol of " Cp^*MoBr_3 ") was reacted with $n\text{-Bu}_4\text{NBr}$ (298 mg, 0.924 mmol) in CH_2Cl_2 . After 1 week, the reaction was complete, as confirmed by $^1\text{H-NMR}$. The brown reaction mixture was filtered and reduced in volume to ca. 5 mL. Addition of diethyl ether (20 mL) induced the formation of a microcrystalline golden precipitate. This was washed with diethyl ether (2 \times 10 mL) and dried *in vacuo*. Yield: 612 mg, 83%. Anal. Calcd for $\text{C}_{26}\text{H}_{51}\text{Br}_4\text{MoN}$: C, 39.37; H, 6.48; N, 1.77. Found: C, 38.93; H, 6.04; N, 1.83. $^1\text{H-NMR}$ (δ , CDCl_3): -19.5 (br, $w_{1/2} = 120$ Hz, Cp^*).

Addition of CO to Various $\text{Cp}^*\text{Mo}-\text{Bromide Systems}$. A 10-mg sample of " Cp^*MoBr_3 " as obtained from the thermal decarbonylation of $\text{Cp}^*\text{MoBr}_3(\text{CO})_2$ in CH_2Cl_2 was introduced into a Schlenk tube with a magnetic stirrer bar and CH_2Cl_2 (3 mL) was added. The mixture was then put under 1 atm of CO. An immediate reaction occurred, and solution IR confirmed the formation of $\text{Cp}^*\text{MoBr}_3(\text{CO})_2$ (2074, 2034 cm^{-1}).

A 50-mg sample of Cp^*MoBr_3 , as obtained from $\text{Cp}^*\text{Mo}_2\text{Br}_4$ and Br_2 in benzene was dissolved in CH_2Cl_2 (5 mL) and then treated with CO as above. In this case, the initially red suspension of the partially soluble starting material did not show any immediate change. Stirring at room temperature overnight under CO, however, led to a color change from red to orange-brown and the development of the solution IR bands assigned to $\text{Cp}^*\text{MoBr}_3(\text{CO})_2$.

Preparation of $\text{Cp}^*\text{MoBr}_3(\text{PMe}_3)$. " Cp^*MoBr_3 " (390 mg, 0.83 mmol) as obtained from the decarbonylation of $\text{Cp}^*\text{MoBr}_3(\text{CO})_2$ in dichloromethane was placed in a Schlenk tube with a magnetic stirrer bar and dissolved in CH_2Cl_2 (10 mL). PMe_3 (86 μL , 0.86 mmol) was added and the orange-brown mixture was stirred at room temperature. No color change was noticed, but a $^1\text{H-NMR}$ spectrum taken on an aliquot after 24 h indicated the complete transformation of all components of the starting material to the product. A crude material was obtained by concentration to a small volume and addition of heptane (5 mL). This was recrystallized from hot toluene (15 mL) to yield 111 mg (20%) of product. Anal. Calcd for $\text{C}_{13}\text{H}_{24}\text{Br}_3\text{MoP}$: C, 28.55; H, 4.4. Found: C, 27.6; H, 4.3. $^1\text{H-NMR}$ (δ , CDCl_3 , room temperature): -4.46 (br, $w_{1/2} = 90$ Hz). $^1\text{H-NMR}$ (δ , CD_2Cl_2 , 206 K): 96.9 (br, $w_{1/2} = 1200$ Hz), -11.13 (br, $w_{1/2} = 260$ Hz), -56.1 (br, $w_{1/2} = 620$ Hz) with a relative intensity of 16.5:60.0:23.5. The variable temperature $^1\text{H-NMR}$ spectrum of this compound has been fully described elsewhere.¹⁵ When an excess amount of PMe_3 was added to a CDCl_3 solution of the compound in the NMR tube, the room temperature $^1\text{H-NMR}$ resonance did not change and no new resonance appeared except for that of free PMe_3 , and the $^{31}\text{P-NMR}$ spectrum showed only the unshifted resonance of free PMe_3 , $\mu_{\text{eff}} = 2.74 \mu_B$ (by the Evans method in CDCl_3/TMS).

Thermal Decarbonylation of $\text{Cp}^*\text{MoI}_3(\text{CO})_2$. (a) In Refluxing Toluene. Preparation of $[\text{Cp}^*\text{Mo}_2(\mu-\text{I})_4]^+(\text{I}^-)_{0.5}(\text{I}_3)^{-0.5}$ (Green Cp^*MoI_3) and Formation of $[\text{Cp}^*\text{Mo}_2(\mu-\text{I})_4]\text{I}_3$. $\text{Cp}^*\text{MoI}_3(\text{CO})_2$ (1.393 g, 2.08 mmol) was refluxed in toluene (10 mL) for 1 day. Heptane (10 mL) was added to the resulting mixture to increase the amount of black (dark green) precipitate, which was then filtered from the purple solution, washed with heptane (20 mL), and dried under vacuum. Yield 1.14 g, 93%. IR analysis on the solid (Nujol mull) revealed the absence of any residual CO. Anal. Calcd for $\text{C}_{10}\text{H}_{15}\text{I}_3\text{Mo}$: C, 19.63; H, 2.47. Found: C, 19.9; H, 2.5. This material was not soluble in aromatic hydrocarbons, but it

(15) Abugideiri, F.; Gordon, J. C.; Poli, R.; Owens-Waltermire, B. E.; Rheingold, A. L. *Organometallics* 1993, 12, 1575.

is sparingly soluble in dichloromethane to afford green solutions. $^1\text{H-NMR}$ (δ , CD_2Cl_2): 2.8 (broad, $w_{1/2} = 50$ Hz).

A recrystallization of this crude product (200 mg) by diffusion of a heptane layer into a CH_2Cl_2 solution afforded ca. 10 mg of well-formed black crystals which were shown by X-ray analysis to consist of $[(\text{Cp}^*\text{Mo})_2(\mu-\text{I})_4]\text{I}_3$. Solutions of this compound in CH_2Cl_2 are deep forest green. Cyclic voltammogram¹³ ($\text{CH}_2\text{Cl}_2/0.1$ M Bu_4NPF_6 , V vs $\text{Cp}_2\text{Fe}/\text{Cp}_2\text{Fe}^+$): -0.381 (reversible reduction, $[(\text{Cp}^*\text{MoI}_2)_2]^+ / (\text{Cp}^*\text{MoI}_2)_2$, $\Delta E_p = 60$ mV), -0.244 (E_{pa}) and -0.116 (E_{pa}) (irreversible reduction, $\text{I}_3^- / \text{I}^-$), +0.212 (reversible oxidation, $\text{I}_3^- / \text{I}^-$, $\Delta E_p = 68$ mV), +0.475 (reversible oxidation, $[(\text{Cp}^*\text{MoI}_2)_2]^+ / (\text{Cp}^*\text{MoI}_2)_2^{2+}$, $\Delta E_p = 60$ mV); the $\text{Cp}_2\text{Fe}/\text{Cp}_2\text{Fe}^+$ couple had $\Delta E_p = 107$ mV. EPR (CH_2Cl_2 , 77 K): $g_\perp = 2.14$; $g_\parallel = 2.35$. Solutions of this compound are EPR silent at room temperature. $^1\text{H-NMR}$ (δ , CD_2Cl_2): 2.8 (broad, $w_{1/2} = 65$ Hz).

(b) In Refluxing Dichloromethane. Preparation of $\text{Cp}_2^*\text{Mo}_2(\mu-\text{I})_2\text{I}_4$ (Purple Cp^*MoI_3). $\text{Cp}^*\text{MoI}_3(\text{CO})_2$ was prepared in situ from $[\text{Cp}^*\text{Mo}(\text{CO})_3]_2$ (1.276 g, 2.024 mmol) and I_2 (1.544 g, 6.083 mmol) in CH_2Cl_2 (50 mL) as described above.^{13,14} After complete conversion as verified by IR spectroscopy (no byproducts are formed in this reaction), the mixture was refluxed for 5 days to afford a black microcrystalline precipitate and a supernatant purple solution. The solid was filtered off and dried under vacuum. IR spectroscopy on this solid (Nujol mull) shows no bands in the CO stretching region. Yield: 1.365 g (55.1%). Anal. Calcd for $\text{C}_{10}\text{H}_{15}\text{I}_3\text{Mo}$: C, 19.63; H, 2.47. Found: C, 20.2; H, 2.8. Contrary to the solid obtained by reflux in toluene, this material slightly dissolves in aromatic hydrocarbons, although not at concentration levels sufficient to observe the $^1\text{H-NMR}$ resonance. The compound is more soluble in chlorinated hydrocarbons to afford dark purple solutions. $^1\text{H-NMR}$ (δ , CD_2Cl_2): -5.1 (br, $w_{1/2} = 17$ Hz). $\mu_{eff} = 1.61 \mu_B$ per Mo atom.

Isomerization of Purple Cp^*MoI_3 to Green Cp^*MoI_3 . The mother liquor of purple Cp^*MoI_3 as obtained as described in the previous section was evaporated to dryness, the residue was slurried in toluene, and the resulting mixture was refluxed for seven days. A green solid formed, which was isolated by filtration and dried under vacuum (280 mg). This material was identified as green Cp^*MoI_3 by comparison of its spectroscopic properties with those of the authentic sample (*vide supra*). In a separate experiment, isolated purple Cp^*MoI_3 (230 mg) was also slurried in toluene and refluxed. After 24 h, the black microcrystalline solid was filtered off, washed with toluene, and dried. This isolated material (95 mg) showed once again solubility and spectroscopic properties identical with those of authentic green Cp^*MoI_3 .

Preparation of $[(\text{Cp}^*\text{Mo})_2(\mu-\text{I})_4]\text{I}_3$. $[\text{Cp}^*\text{Mo}(\text{CO})_2]$ (538 mg, 0.85 mmol) and I_2 (758 mg, 2.99 mmol) were placed in a Schlenk tube with a magnetic stirrer bar. CH_2Cl_2 (10 mL) was added, and the resulting mixture was stirred overnight. The formation of the sparingly soluble $\text{Cp}^*\text{MoI}_3(\text{CO})_2$ was confirmed by IR in the CO stretching region. The tube was then fitted with a reflux condenser and the mixture refluxed for 2 days, to produce a large amount of black microcrystalline precipitate in a purple solution. The solid was collected by filtration, washed with CH_2Cl_2 (3×10 mL), and dried under vacuum. The last washing had a deep green color. Yield: 0.929 g, 81%. The identity of this compound as the salt $[(\text{Cp}^*\text{Mo})_2(\mu-\text{I})_4]\text{I}_3$ was confirmed by $^1\text{H-NMR}$ and cyclic voltammetry.

Conversion of $[\text{Cp}_2^*\text{Mo}_2(\mu-\text{I})_4]^+(\text{I}^-)_0\text{S}(\text{I}_3^-)_0\text{S}$ to $[\text{Cp}_2^*\text{Mo}_2(\mu-\text{I})_4]\text{I}_3$. The product from the decarbonylation of $\text{Cp}^*\text{MoI}_3(\text{CO})_2$ in toluene, green Cp^*MoI_3 (100 mg, 0.08 mmol), was placed in a Schlenk tube and suspended in CH_2Cl_2 . I_2 (11 mg, 0.04 mmol) was added, causing the dissolution of most of the starting material and the formation of a dark green solution. After being stirred at room temperature for 4 days, the solution was filtered and the solid was washed with CH_2Cl_2 (2 mL). The combined solutions were evaporated to dryness. The resulting residue was confirmed to be the salt $[(\text{Cp}^*\text{Mo})_2(\mu-\text{I})_4]\text{I}_3$ by $^1\text{H-NMR}$, cyclic voltammetry, and analytical data. Anal. Calcd for $\text{C}_{20}\text{H}_{30}\text{I}_3\text{Mo}$: C, 17.78; H, 2.24. Found: C, 18.0; H, 2.3. An analogous transformation was observed when starting from purple Cp^*MoI_3 , i.e. the product of decarbonylation of $\text{Cp}^*\text{MoI}_3(\text{CO})_2$ in CH_2Cl_2 .

Reaction of $[\text{Cp}_2^*\text{Mo}_2(\mu-\text{I})_4]\text{I}_3$ with PMe_3 . Preparation and Characterization of $\text{Cp}_2^*\text{Mo}_2\text{I}_4$. This reaction is a slight modification of a procedure for the preparation of $\text{Cp}_2^*\text{Mo}_2\text{I}_4$ discovered by Parkin.¹⁶ $[(\text{Cp}^*\text{Mo})_2(\mu-\text{I})_4]\text{I}_3$ is slurried in THF and treated with 1.5 mol/mol of PMe_3 . Stirring at room temperature for 45 min results in a color change from green to orange-brown and precipitation of a white solid. After filtration, the volume of the solution is reduced by evaporation under

reduced pressure. Overnight storage at -20 °C produces the crystalline product as a brown solid in yields up to 96%. $^1\text{H-NMR}$ (δ , CDCl_3): 2.11 (s). Cyclic voltammetry ($\text{CH}_2\text{Cl}_2/0.1$ M Bu_4NPF_6 , V vs $\text{Cp}_2\text{Fe}/\text{Cp}_2\text{Fe}^+$): -0.384 (reversible oxidation, $[(\text{Cp}^*\text{MoI}_2)_2]^+ / (\text{Cp}^*\text{MoI}_2)_2$, $\Delta E_p = 82$ mV), +0.492 (reversible oxidation, $[(\text{Cp}^*\text{MoI}_2)_2]^+ / (\text{Cp}^*\text{MoI}_2)_2^{2+}$, $\Delta E_p = 88$ mV); the $\text{Cp}_2\text{Fe}/\text{Cp}_2\text{Fe}^+$ couple had $\Delta E_p = 82$ mV.

Parkin's procedure differs from that reported here in that it utilizes as starting materials green Cp^*MoI_3 and PMe_3 in a 2:1 Mo/P ratio. The reaction between $\text{Cp}_2^*\text{Mo}_2\text{I}_6$ (purple Cp^*MoI_3) and PMe_3 in a 2:1 Mo/P ratio also gave rise to the formation of $\text{Cp}_2^*\text{Mo}_2\text{I}_4$ as the main product according to $^1\text{H-NMR}$, but other paramagnetic products were also produced (resonances at δ -11.8, -17.4, and -21.1) and the reaction was not investigated further.

Reaction between $\text{Cp}_2^*\text{Mo}_2\text{I}_4$ and AgPF_6 . Preparation of $[\text{Cp}_2^*\text{Mo}_2\text{I}_4]\text{PF}_6$. $[\text{Cp}^*\text{MoI}_2]_2$ (620 mg, 0.64 mmol) was placed in a Schlenk tube with a magnetic stirrer bar and dissolved in CH_2Cl_2 (20 mL) to produce a yellow-green solution. AgPF_6 (162 mg, 0.64 mmol) was added to produce an instantaneous color deepening while a gray precipitate formed. After 2 h stirring at room temperature, the deep forest green solution was filtered and the precipitate was washed with CH_2Cl_2 (3×10 mL). The combined solutions were evaporated to dryness, to yield 532 mg, 75%, of the microcrystalline dark green product. Anal. Calcd for $\text{C}_{20}\text{H}_{30}\text{F}_6\text{I}_4\text{Mo}_2\text{P}$: C, 21.54; H, 2.71. Found: C, 21.9; H, 2.9. Cyclic voltammogram ($\text{CH}_2\text{Cl}_2/0.1$ M Bu_4NPF_6 , V vs $\text{Cp}_2\text{Fe}/\text{Cp}_2\text{Fe}^+$): -0.387 (reversible reduction, $[(\text{Cp}^*\text{MoI}_2)_2]^+ / (\text{Cp}^*\text{MoI}_2)_2$, $\Delta E_p = 77$ mV), +0.480 (reversible oxidation, $[(\text{Cp}^*\text{MoI}_2)_2]^+ / (\text{Cp}^*\text{MoI}_2)_2^{2+}$, $\Delta E_p = 87$ mV); the $\text{Cp}_2\text{Fe}/\text{Cp}_2\text{Fe}^+$ couple had $\Delta E_p = 59$ mV. $^1\text{H-NMR}$ (δ , CD_2Cl_2): 2.7 (broad, $w_{1/2} = 40$ Hz). $^{31}\text{P-NMR}$ (δ , CD_2Cl_2): -143.75 (septet, $J_{FP} = 711$ Hz).

Attempts To Synthesize $[\text{Cp}_2^*\text{Mo}_2\text{I}_4](\text{PF}_6)_2$. $[(\text{Cp}^*\text{MoI}_2)_2]$ (445 mg, 0.40 mmol) was dissolved in 30 mL of CH_2Cl_2 , and to the resulting stirred solution was added AgPF_6 (101 mg, 0.40 mmol). The formation of a gray precipitate immediately ensued, but the color of the solution did not change. After 1 h of stirring at room temperature, the solution was filtered and an aliquot withdrawn for NMR inspection in CD_2Cl_2 . The $^1\text{H-NMR}$ spectrum showed only the resonance of the starting material. An additional equivalent of AgPF_6 was then added by maintaining the solution at -30 °C. Again, a gray precipitate formed immediately, but the color and the $^1\text{H-NMR}$ spectrum of the solution did not change. The solution was then filtered and evaporated to dryness. The residue was taken up in MeCN to yield a deep green solution. This solution was in turn evaporated to dryness and the residue dissolved once again in MeCN (30 mL). After filtration, 100 mg of AgPF_6 were added. A gray precipitate formed immediately, but the color and the $^1\text{H-NMR}$ spectrum of the solution again indicated that $[\text{Cp}_2^*\text{Mo}_2\text{I}_4]^+$ was the only Cp^* -containing species present in solution.

Reaction between Cp^*MoI_3 and AgPF_6 . (a) From Green Cp^*MoI_3 . Green Cp^*MoI_3 as obtained from the toluene reflux (490 mg, 0.80 mmol) was placed in a Schlenk tube with a magnetic stirrer bar and suspended in CH_2Cl_2 (15 mL). The solution became green while most of the solid remained undissolved. AgPF_6 (203 mg, 0.80 mmol) was added, and the mixture was stirred at room temperature. A rapid deepening of the green color was observed, while a pale precipitate replaced the dark starting solid. A $^1\text{H-NMR}$ spectrum on an aliquot of the solution showed that the $[\text{Cp}_2^*\text{Mo}_2\text{I}_4]^+$ cation was the only proton-containing species in solution (δ 2.74, $w_{1/2} = 60$ Hz in CDCl_3).

(b) From Purple Cp^*MoI_3 . A purple solution of the Cp^*MoI_3 material obtained from the methylene chloride reflux gave a more complex reaction, with more than one product being obtained as shown by $^1\text{H-NMR}$ on an aliquot of the resulting brown solution. The formation of a gray precipitate (presumably metallic Ag) was also observed. However, $^1\text{H-NMR}$ and cyclic voltammetry indicated the presence of the $[\text{Cp}_2^*\text{Mo}_2\text{I}_4]^+$ cation.

Reaction between $[\text{Cp}^*\text{MoCl}_2]_2$ and HI. Crystallization of $[\text{Cp}_2^*\text{Mo}_2(\mu-\text{Cl})_x(\mu-\text{I})_{4-x}]_3$. $[\text{Cp}^*\text{MoCl}_2]_2$ (1.418 g, 2.35 mmol) was introduced in a Schlenk tube containing a magnetic stirrer bar and dissolved in CH_2Cl_2 (50 mL). Anhydrous HI(g) was bubbled through the solution for 2 h at room temperature. The color of the solution changed from brown to deep forest green while a dark microcrystalline precipitate formed. The mixture was evaporated to dryness and the residue was washed with toluene (30 mL) followed by pentane (2×10 mL). These washings were colorless. The solid was dried under vacuum. Yield 2.551 g. This solid had similar but not identical properties compared with those of the salt $[\text{Cp}_2^*\text{Mo}_2\text{I}_4]\text{I}_3$ described above. $^1\text{H-NMR}$ (δ , CD_2Cl_2): 4.6 (broad, $w_{1/2} = 100$ Hz). CV ($\text{CH}_2\text{Cl}_2/0.1$ M Bu_4NPF_6 , V vs $\text{Cp}_2\text{Fe}/\text{Cp}_2\text{Fe}^+$): ca. -0.35 (reversible 1-e reduction), -0.152 (E_{pa}) (irreversible $\text{I}_3^- / \text{I}^-$) (the cathodic peak of this couple, at ca. -0.42 V, overlapped with the reduction wave of the reversible couple at $E_{1/2} =$

(16) (a) Parkin, G. Personal communication, August 1992. (b) Shin, J. H.; Parkin, G. *Polyhedron* 1994, 13, 1489.

Table 1. Crystal Data for All Compounds

	$\text{Cp}^*\text{Mo}_2\text{Br}_6$ (1)	$\text{Cp}^*\text{Mo}_2\text{Br}_6$ (2)	$\text{Cp}^*\text{Mo}_2\text{Br}_6 \cdot$ C_6H_6	$\text{Cp}^*\text{Mo}_2\text{Br}_4$	$[\text{Cp}^*\text{Mo}_2\text{Br}_4]_2 \cdot$ $2\text{C}_7\text{H}_{16}$	$[\text{Cp}^*\text{MoBr}_4]_3 \cdot$	$[\text{Cp}^*\text{Mo}_2\text{I}_4] \cdot$ I_3	$[\text{Cp}^*\text{Mo}_2\text{Cl}_x\text{I}_{4-x}] \cdot$ I_3	$[\text{NMe}_3\text{Ph}] \cdot$ $[\text{Cp}^*\text{MoI}_4]$
formula	$\text{C}_{20}\text{H}_{30}\text{Br}_6\text{Mo}_2$	$\text{C}_{20}\text{H}_{30}\text{Br}_6\text{Mo}_2$	$\text{C}_{26}\text{H}_{36}\text{Br}_6\text{Mo}_2$	$\text{C}_{20}\text{H}_{30}\text{Br}_4\text{Mo}_2$	$\text{C}_{84}\text{H}_{137}\text{Br}_{20}\text{Mo}_7$	$\text{C}_{20}\text{H}_{30}\text{I}_7\text{Mo}_2$	$\text{C}_{20}\text{H}_{30}\text{Cl}_x\text{I}_{7-x}\text{Mo}_2$	$\text{C}_{19}\text{H}_{29}\text{I}_4\text{MoN}$	
fw	941.76	941.76	1019.87	782.0	3416.67	1350.67	1167.7 ($x = 2$)	875.00	
space group	$C2/c$	$P2_1/n$	$P2_1/n$	$P2_1/n$	$P2_1/m$	$Cmc2_1$	$Pn2_1a$	$P2_1/c$	
$a, \text{\AA}$	15.104(8)	8.624(1)	9.173(6)	8.356(1)	20.218(6)	11.756(3)	22.041(8)	9.270(2)	
$b, \text{\AA}$	8.450(4)	13.600(2)	16.595(4)	32.272(5)	23.332(5)	14.103(4)	11.891(3)	18.456(15)	
$c, \text{\AA}$	21.591(13)	11.411(2)	10.538(3)	13.972(2)	12.093(2)	18.696(5)	11.771(3)	29.936(6)	
β, deg	100.82(4)	92.73(1)	92.52(4)	98.17(1)	104.76(2)			95.29(2)	
$V, \text{\AA}^3$	2707(3)	1336.8(4)	1602(2)	3729.3(10)	5516(2)	3100.0(14)	3085.4(16)	5100(6)	
Z	4	2	2	6	2	4	4	8	
$d_{\text{calc}}, \text{g/cm}^3$	2.31	2.34	2.11	2.088	2.06	2.894	2.828	2.32	
$\mu(\text{Mo K}\alpha), \text{cm}^{-1}$	97.91	99.11	87.03	73.60	84.62	106.7	134.94	54.69	
radiation	(monochromated Mo K α ($\lambda = 0.71073 \text{\AA}$) in incident beam)								
temp, $^{\circ}\text{C}$	26	-29	23	25	25	23	25	23	
$T_{\text{max}}/T_{\text{min}}$	2.10	1.15	4.37	1.81	4.5	3.35	1.33	3.33	
R^a	0.054	0.050	0.056	0.061	0.089	0.042	0.062	0.055	
R_w^b	0.070	0.061	0.080	0.076	0.094	0.045	0.088	0.068	

$$^a R = \sum |F_o| - |F_c| / \sum |F_o|. \quad ^b R_w = [\sum w(|F_o| - |F_c|)^2 / \sum w|F_o|^2]^{1/2}; w = 1/\sigma^2(|F_o|).$$

-0.35 V), +0.244 (reversible I_3^-/I_2 , $\Delta E_p = 95 \text{ mV}$), +0.585 (reversible 1-e oxidation, $\Delta E_p = 55 \text{ mV}$); the $\text{Cp}_2\text{Fe}/\text{Cp}_2\text{Fe}^+$ couple had $\Delta E_p = 73 \text{ mV}$.

In a similar preparation starting from 218 mg (0.36 mmol) of $[\text{Cp}^*\text{MoCl}_2]_2$ in 20 mL of CH_2Cl_2 , the solution obtained after HI bubbling for 5 min at -20 °C was filtered and set for crystallization by diffusion of a toluene layer. A total of 223 mg of large crystals was recovered. $^1\text{H-NMR}$ (δ , CD_2Cl_2): 4.6 (broad, $w_{1/2} = 60 \text{ Hz}$). One crystal was investigated by X-ray diffraction (vide infra) and found to correspond to the compositionally disordered $[\text{Cp}^*\text{Mo}_2(\mu\text{-Cl})_x(\mu\text{-I})_{4-x}] \text{I}_3$ ($x = \text{ca. } 2$ by refinement of X-ray data). Anal. Calcd for $\text{C}_{20}\text{H}_{30}\text{Cl}_2\text{I}_5\text{Mo}_2$: C, 20.57; H, 2.59. Found: C, 20.0; H, 2.4.

Reaction of Cp^*MoI_3 with I⁻. (a) **From Green Cp^*MoI_3 .** Green Cp^*MoI_3 (216 mg, 0.353 mmol) and *n*-Bu₄NI (121 mg, 0.328 mmol) were introduced into a Schlenk tube and then dichloromethane (10 mL) was added. The mixture was stirred at room temperature for 1 day, after which time an aliquot of the solution was withdrawn and inspected by $^1\text{H-NMR}$ (CDCl_3). Only the resonances of the *n*-Bu₄N⁺ cation and of the Mo starting material were observed.

(b) **From Purple Cp^*MoI_3 . Preparation of $[\text{Cp}^*\text{MoI}_4]^-$.** Purple Cp^*MoI_3 (441 mg, 0.721 mmol) was dissolved in CH_2Cl_2 (20 mL), and to the resulting purple solution was added *n*-Bu₄NI (269 mg, 0.728 mmol). The solution turned immediately from purple to dark green. The solution was reduced in volume to ca. 5 mL, and pentane (20 mL) was added causing the formation of a dark green precipitate. The supernatant liquid was decanted off and the precipitate was washed with pentane (2 × 20 mL) and dried under vacuum. Yield: 343 mg (49%). Anal. Calcd for $\text{C}_{26}\text{H}_{51}\text{I}_4\text{MoN}$: C, 31.83; H, 5.24. Found: C, 31.9; H, 5.5. $^1\text{H-NMR}$ (δ , CDCl_3 , room temperature): -21.7 (br, $w_{1/2} = 60 \text{ Hz}$).

From an analogous reaction between equimolar amounts of purple Cp^*MoI_3 (211 mg, 0.344 mmol) and NMe_3PhI^- (91 mg, 0.345 mmol) in CH_2Cl_2 , a dark green solution formed immediately. Crystallization from $\text{CH}_2\text{Cl}_2/\text{heptane}$ (5 mL/50 mL) afforded 103 mg (34% yield) of dark green needles, whose $^1\text{H-NMR}$ spectrum at room temperature (CDCl_3) showed a broad peak at -21.1 ppm, consistent with the presence of the $[\text{Cp}^*\text{MoI}_4]^-$ ion. A single crystal from this batch was used for the X-ray analysis.

Reactions of Cp^*MoI_3 and of $[\text{Cp}^*\text{Mo}_2\text{I}_4]\text{I}_3$ with CO. The purple Cp^*MoI_3 isolated from the dichloromethane reflux procedure (43 mg, 0.07 mmol) was dissolved in CH_2Cl_2 (10 mL) and subsequently exposed to CO (1 atm). The solution rapidly changed color from purple to brown. An IR of the solution confirmed that the formation of $\text{Cp}^*\text{MoI}_3(\text{CO})_2$ had occurred.

An analogous experiment was carried out on a solution of green Cp^*MoI_3 which had been isolated from the toluene reflux procedure. After 24 h of exposure to CO at 1 atm, the solution remained green and IR spectroscopy did not show the formation of carbonyl products.

An analogous experiment was carried out on a CH_2Cl_2 solution of $[\text{Cp}^*\text{Mo}_2\text{I}_4]\text{I}_3$. No change was noted over a period of 5 days stirring at room temperature under 1 atm of CO, and no IR absorptions were observed for the solution in the carbonyl stretching region.

X-ray Crystallography. General Data. In each case, a crystal suitable for an X-ray structural investigation was mounted on the tip of a glass

Table 2. Atomic Coordinates ($\times 10^5$) and Equivalent Isotropic Displacement Coefficients ($\text{\AA}^2 \times 10^4$) for $\text{Cp}^*\text{Mo}_2\text{Br}_6$ (Polymorphs 1 and 2)

	<i>x</i>	<i>y</i>	<i>z</i>	<i>U</i> (eq) ^a
(a) Polymorph 1				
Mo	7361(1)	2115(2)	5913(1)	25(1)
Br(1)	8457(1)	18(2)	6419(1)	53(1)
Br(2)	6144(1)	77(2)	5950(1)	56(1)
Br(3)	6413(1)	2570(2)	4786(1)	40(1)
C(1)	7508(12)	4877(19)	6087(7)	41(6)
C(2)	8091(10)	4070(20)	6572(9)	42(7)
C(3)	7585(11)	3202(20)	6934(7)	41(6)
C(4)	6677(11)	3442(21)	6670(8)	44(7)
C(5)	6642(12)	4453(23)	6162(8)	50(7)
C(6)	7740(16)	6001(24)	5630(10)	92(12)
C(7)	9131(12)	4300(29)	6730(11)	96(11)
C(8)	7921(16)	2367(26)	7532(8)	99(12)
C(9)	5899(14)	2848(28)	6961(11)	102(12)
C(10)	5752(16)	5111(30)	5781(12)	141(15)
(b) Polymorph 2				
Mo	4847(11)	47395(7)	67362(8)	141(3)
Br(1)	-19036(16)	49531(12)	79207(12)	444(5)
Br(2)	14696(19)	62901(10)	77182(13)	454(5)
Br(3)	-16450(15)	44197(10)	50889(11)	312(4)
C(1)	15578(137)	32398(74)	61878(97)	229(36)
C(2)	5167(125)	30587(78)	70884(100)	197(34)
C(3)	11603(131)	34903(82)	81304(97)	226(35)
C(4)	25425(122)	39637(77)	78979(95)	192(34)
C(5)	28201(130)	38118(78)	66956(94)	208(34)
C(6)	14650(155)	28199(93)	49899(109)	387(46)
C(7)	-8777(136)	24028(92)	70086(116)	360(45)
C(8)	5315(167)	33596(119)	93440(102)	474(53)
C(9)	36439(151)	44345(99)	87854(114)	398(46)
C(10)	42849(145)	40656(110)	60993(123)	438(51)

^a Equivalent isotropic *U* defined as one-third of the trace of the orthogonalized U_{ij} tensor.

fiber with epoxy cement. Selected crystal, data collection and refinement parameters for all compounds are collected in Table 1. The unit cell parameters and the orientation matrix for data collection were obtained from the least-squares fit of the setting angles of 25 reflections. In each case, the data were corrected for Lorentz and polarization factors, and for absorption by the semiempirical ψ -scan method. All structures were solved by direct methods which located the heavy atoms, and the remaining non-hydrogen atoms were located by alternating full-matrix least-squares refinement and difference Fourier syntheses. All hydrogen atoms were included as idealized isotropic contributions ($d(\text{CH}) = 0.960 \text{ \AA}$, $U = 1.2U$ for attached C). Unless otherwise stated, all non-hydrogen atoms were refined with anisotropic thermal parameters. The software used and the sources of the scattering factors are contained in the SHELXTLPLUS(4.2) program library^{17a} for structures described in sections (a), (c), and (e), and in the TEXSAN program library^{17b} for structures described in sections (b), (d), (f), and (g).

Table 3. Selected Bond Distances (\AA) and Angles (deg) for $\text{Cp}^*\text{Mo}_2\text{Br}_6$

	polymorph 1	polymorph 2	$\text{Cp}^*\text{Mo}_2\text{Br}_6\text{C}_6\text{H}_6$
(a) Distances ^a			
Mo-Br(1)	2.529(2)	2.534(2)	2.537(3)
Mo-Br(2)	2.531(2)	2.517(2)	2.531(3)
MoBr(3)	2.610(2)	2.601(2)	2.623(3)
Mo-Br(3a)	2.616(2)	2.616(2)	2.627(3)
Mo-CNT	2.034(19)	2.036(11)	2.02(2)
Mo...Mo	4.094(2)	4.073(2)	4.126(3)
(b) Angles ^a			
Br(1)-Mo-Br(2)	86.0(1)	86.1(1)	86.6(1)
Br(1)-Mo-Br(3)	134.9(1)	80.8(1)	134.1(1)
Br(1)-Mo-Br(3a)	81.0(1)	136.6(1)	81.1(1)
Br(1)-Mo-CNT	112.9(4)	112.6(3)	112.1(5)
Br(2)-Mo-Br(3)	81.7(1)	132.3(1)	81.2(1)
Br(2)-Mo-Br(3a)	133.2(1)	81.6(1)	133.8(1)
Br(2)-Mo-CNT	113.6(5)	114.2(3)	112.6(5)
Br(3)-Mo-Br(3a)	76.7(1)	77.4(1)	76.38(8)
Br(3)-Mo-CNT	111.8(4)	113.2(3)	113.4(5)
Br(3a)-Mo-CNT	112.9(4)	110.5(3)	113.2(5)
Mo-Br(3)-Mo'	103.3(1)	102.6(1)	103.62(8)

^a CNT = centroid of atoms C(1) to C(5).

Table 4. Positional Parameters and $B(\text{eq})$ for $\text{Cp}^*\text{Mo}_2\text{Br}_6\text{C}_6\text{H}_6$

atom	x	y	z	$B(\text{eq}), \text{\AA}^2$
Mo	0.4502(2)	0.11667(8)	0.4462(2)	3.33(7)
Br(1)	0.3837(3)	0.1989(1)	0.6381(2)	6.2(1)
Br(2)	0.6805(3)	0.2006(1)	0.4443(3)	6.6(1)
Br(3)	0.6383(2)	0.0009(1)	0.4091(2)	5.0(1)
C(1)	0.304(2)	0.065(1)	0.278(2)	4(1)
C(2)	0.213(2)	0.115(1)	0.357(2)	3.9(9)
C(3)	0.261(2)	0.196(1)	0.345(2)	4(1)
C(4)	0.387(2)	0.196(1)	0.263(2)	4(1)
C(5)	0.407(2)	0.117(1)	0.228(2)	4(1)
C(6)	0.281(3)	-0.022(1)	0.248(2)	6(1)
C(7)	0.081(2)	0.089(1)	0.419(3)	7(1)
C(8)	0.187(2)	0.270(1)	0.393(2)	6(1)
C(9)	0.456(3)	0.270(1)	0.219(3)	7(1)
C(10)	0.517(3)	0.093(1)	0.132(2)	6(1)
C(11)	0.931(3)	0.044(2)	0.084(3)	8.6(7)
C(12)	1.031(3)	0.077(2)	0.011(3)	7.4(6)
C(13)	0.904(4)	-0.032(2)	0.077(3)	9.5(8)

^a For anisotropically refined atoms, $B(\text{eq})$ is defined as one-third of the trace of the orthogonalized \mathbf{B}_{ij} tensor.

(a) $\text{Cp}^*\text{Mo}_2\text{Br}_6$. Two polymorphs were investigated for this compound. The systematic absences from the data uniquely established the space group as $C2/c$ for polymorph 1, and $P2_1/n$ for 2. For both polymorphs, positional parameters are reported in Table 2 and selected bond distances and angles are reported in Table 3.

(b) $\text{Cp}^*\text{Mo}_2\text{Br}_6\text{C}_6\text{H}_6$. This compound gave a monoclinic unit cell by indexing on 20 out of 25 centered reflections found by a random search. Axial photographs confirmed the $2/m$ Laue class but showed interlayers along the a and c axes, whereas no interlayers spots were noticed along the b axis, indicating that the crystal was twinned with one or more minor orientations aligned with the major one in a parallel fashion along the b axis but in a random fashion along the other two directions. Data were collected on the reflections of the major orientation. Careful scrutiny of the data set showed no evidence of accidental overlap with reflections of the minor components. The systematic absences uniquely established the space group as $P2_1/n$. Positional parameters are reported in Table 4 and selected bond distances and angles are compared with those of the two $\text{Cp}^*\text{Mo}_2\text{Br}_6$ polymorphs in Table 3.

(c) $\text{Cp}^*\text{Mo}_2\text{Br}_4$. The systematic absences from the data uniquely established the space group as $P2_1/n$. The asymmetric unit contains one and a half molecules which are chemically similar but crystallographically independent, with the half molecule located on a crystallographic inversion center. Positional parameters are listed in Table 5 and selected bond distances and angles are reported in Table 6.

(d) $[(\text{Cp}^*\text{Mo}_2\text{Br}_4)]^4[\text{Cp}^*\text{MoBr}_4]_2\text{Cp}^*\text{MoBr}_4\text{C}_2\text{H}_{16}$. The systematic absences indicated either space group $P2_1$ or $P2_1/m$. The centrosymmetric

Table 5. Atomic Coordinates ($\times 10^4$) and Equivalent Isotropic Displacement Coefficients ($\text{\AA}^2 \times 10^3$) for $\text{Cp}^*\text{Mo}_2\text{Br}_4$

	x	y	z	$U(\text{eq})^a$
Mo(1)	419(2)	213(1)	4268(1)	27(1)
Mo(2)	3758(2)	2031(1)	10979(1)	29(1)
Mo(3)	2605(2)	1421(1)	9815(1)	27(1)
Br(1)	-2194(3)	-245(1)	4042(2)	62(1)
Br(2)	-1463(3)	548(1)	5408(2)	62(1)
Br(3)	2928(5)	1330(1)	11685(2)	104(2)
Br(4)	652(3)	1965(1)	10398(3)	97(1)
Br(5)	3417(4)	2123(1)	9100(2)	83(1)
Br(6)	5698(3)	1487(1)	10376(3)	88(1)
C(1)	724(28)	835(6)	3556(14)	38(8)
C(2)	2244(26)	673(8)	3647(15)	48(9)
C(3)	2136(24)	290(6)	3165(16)	38(8)
C(4)	528(28)	234(7)	2701(15)	44(8)
C(5)	-395(24)	586(8)	2957(15)	42(8)
C(6)	327(37)	1267(7)	3961(20)	94(15)
C(7)	3799(29)	846(9)	4196(20)	102(14)
C(8)	3493(35)	23(9)	3011(22)	128(17)
C(9)	-116(34)	-94(8)	1981(17)	90(13)
C(10)	-2120(30)	697(8)	2611(18)	81(12)
C(11)	4538(32)	2264(6)	12536(15)	46(9)
C(12)	3352(24)	2528(6)	12088(14)	35(8)
C(13)	3983(28)	2711(6)	11283(14)	41(8)
C(14)	5544(25)	2541(7)	11248(17)	48(9)
C(15)	5878(30)	2288(7)	12039(17)	53(10)
C(16)	4405(39)	2051(9)	13474(17)	102(15)
C(17)	1701(29)	2628(10)	12405(19)	96(15)
C(18)	3193(30)	3041(7)	10624(18)	75(12)
C(19)	6719(27)	2673(8)	10600(17)	67(11)
C(20)	7464(27)	2035(7)	12369(21)	89(13)
C(21)	3086(23)	893(6)	8783(15)	33(7)
C(22)	1974(26)	1166(7)	8216(15)	42(6)
C(23)	580(23)	1176(7)	8724(15)	42(8)
C(24)	890(25)	913(6)	9546(14)	36(8)
C(25)	2413(25)	743(6)	9570(15)	40(8)
C(26)	4661(27)	773(8)	8493(17)	79(12)
C(27)	2130(31)	1380(8)	7319(17)	71(11)
C(28)	-1012(28)	1403(8)	8296(16)	73(11)
C(29)	-438(26)	801(7)	10176(15)	54(9)
C(30)	3160(29)	399(7)	10282(15)	61(10)

^a Equivalent isotropic U defined as one-third of the trace of the orthogonalized \mathbf{U}_{ij} tensor.

choice was first selected on the basis of intensity statistics. The structure could not be solved by either direct method solutions (MITHRIL) nor by the automatic Patterson map interpretation program available in the TEXSAN package.^{17b} Every tentative solution indicated the presence of a quadruply-bromo-bridged dimolybdenum unit and of one or more pyramidal MoBr₄ arrangement with distances and angles typical of four-legged piano-stool geometries, but each attempt to bring these to refinement failed. The number and correct positioning of these units were established by lowering the symmetry to $P1$ and by using the Mo-(μ -Br)₄Mo unit as obtained from the $\text{Cp}^*\text{Mo}_2\text{Br}_4$ structure as input for the programs ORIENT and DIRIF. The positions of all Mo atoms and most of the Br atoms were obtained and refined in $P1$ to $R = 19.9\%$. Increase of symmetry to $P2_1$ allowed the location of the remaining Br atoms and a refinement to $R = 15.5\%$. At this point the mirror plane was introduced by changing the space group to $P2_1/m$ and refinement continued. The remaining atoms were located, including the interstitial heptane molecule, but a stable convergence could not be achieved when the positions of the lighter carbon atoms were allowed to refine freely. The refinement was then continued with all Cp* ligands restrained to ideal pentagons with C-C(ring) = 1.42(1) \AA and C-C(Me) = 1.56(5) \AA , and the interstitial heptane molecule restrained to C-C = 1.54(2) \AA . A few Cp* methyl C atoms refined with a very high thermal parameter, consistent with a pronounced thermal motion by ring whizzing and/or partial disorder of the rings among different orientations. Unfortunately the amount of data did not permit the anisotropic refinement of these atoms. The heptane C atoms also refined with very high thermal parameters indicating possible disorder with other orientations, but we failed to clearly identify a disorder model. The final difference Fourier map showed several peaks with a height between 1 and 2 e/ \AA^3 between the molybdenum atoms of the dimeric unit (Mo(2) and Mo3), in positions that would seem reasonable for one or more additional orientations of the central Mo(μ -Br)₄Mo unit. However, the introduction of the four most

(17) (a) Sheldrick, G., Siemens XRD, Madison, WI. (b) Molecular Structure Corporation, Houston, TX. (c) Rogers, D. *Acta Crystallogr.* 1981 **A27**, 734.

Table 6. Selected Bond Distances (\AA) and Angles (deg) for $\text{Cp}^*{}_{\text{2}}\text{Mo}_2\text{Br}_4$

(a) Distances ^a			
Mo(2)-Mo(3)	2.645(2)	Mo(1)-Mo(1a)	2.641(4)
Mo(2)-Br(3)	2.601(4)	Mo(1)-Br(1)	2.618(3)
Mo(2)-Br(4)	2.615(3)	Mo(1)-Br(2)	2.625(3)
Mo(2)-Br(5)	2.617(3)	Mo(1)-Br(1a)	2.606(3)
Mo(2)-Br(6)	2.609(4)	Mo(1)-Br(2a)	2.625(3)
Mo(3)-Br(3)	2.606(3)	Mo(3)-Br(4)	2.605(4)
Mo(3)-Br(5)	2.604(3)	Mo(3)-Br(6)	2.600(3)
Mo(2)-CNT(2)	1.93(2)	Mo(1)-CNT(1)	1.93(2)
Mo(2)-CNT(3)	1.92(2)		
(b) Angles ^a			
Br(3)-Mo(2)-Br(5)	118.9(1)	Br(1)-Mo(1)-Br(1a)	119.3(1)
Br(4)-Mo(2)-Br(6)	118.7(1)	Br(2)-Mo(1)-Br(2a)	119.6(1)
Br(3)-Mo(3)-Br(5)	119.2(1)	Br(4)-Mo(3)-Br(6)	119.4(1)
Br(3)-Mo(2)-Br(4)	75.0(1)	Br(1)-Mo(1)-Br(2)	75.2(1)
Br(3)-Mo(2)-Br(6)	75.5(1)	Br(1)-Mo(1)-Br(2a)	75.3(1)
Br(4)-Mo(2)-Br(5)	74.7(1)	Br(1a)-Mo(1)-Br(2)	75.3(1)
Br(5)-Mo(2)-Br(6)	74.7(1)	Br(1a)-Mo(1)-Br(2a)	75.4(1)
Br(3)-Mo(3)-Br(4)	75.1(1)	Br(3)-Mo(3)-Br(6)	75.5(1)
Br(4)-Mo(3)-Br(5)	75.1(1)	Br(5)-Mo(3)-Br(6)	75.1(1)
Mo(3)-Mo(2)-CNT(2)	178.3(6)	Mo(1a)-Mo(1)-CNT(1)	179.5(5)
Mo(2)-Mo(3)-CNT(3)	179.5(6)	Br(3)-Mo(2)-CNT(2)	119.9(6)
Br(1)-Mo(1)-CNT(1)	121.0(6)	Br(4)-Mo(2)-CNT(2)	122.3(6)
Br(2)-Mo(1)-CNT(1)	120.4(6)	Br(5)-Mo(2)-CNT(2)	121.2(6)
Br(1a)-Mo(1)-CNT(1)	119.7(6)	Br(6)-Mo(2)-CNT(2)	119.0(6)
Br(2a)-Mo(1)-CNT(1)	120.0(6)	Br(3)-Mo(3)-CNT(3)	120.8(5)
Br(4)-Mo(3)-CNT(3)	120.7(6)	Br(5)-Mo(3)-CNT(3)	120.1(5)
Br(6)-Mo(3)-CNT(3)	119.9(6)	Mo(2)-Br(3)-Mo(3)	61.1(1)
Mo(1)-Br(1)-Mo(1a)	60.7(1)	Mo(2)-Br(4)-Mo(3)	60.9(1)
Mo(1)-Br(2)-Mo(1a)	60.4(1)	Mo(2)-Br(5)-Mo(3)	60.9(1)
Mo(2)-Br(6)-Mo(3)	61.0(1)		

^a CNT = centroid of the Cp^* ring.

prominent peaks with restrained distances ($\text{Mo}-\text{Br} = 2.64(2)$ \AA , *cis*- $\text{Br}-\text{Br} = 3.24(2)$ \AA) and refinement of the occupancy factor led to an occupancy of zero for this second orientation and an occupancy of one for the main orientation of the four bridging bromine atoms. The final agreement factor is 0.089. Possible causes for the difficult refinement of this structure are the very irregular shape of the crystal and the consequent severe absorption ($T_{\max}/T_{\min} = 4.5$) whose correction by the ψ -scan method may have been inaccurate, the great thermal motion and/or partial disorder in the Cp^* ligands and in the interstitial heptane molecule, and the possible slight disorder of the $\text{Mo}(\mu-\text{Br})_4\text{Mo}$ unit. Positional parameters are listed in Table 7 and selected bond distances and angles are given in Table 8.

(e) $[\text{Cp}^*{}_{\text{2}}\text{Mo}_2(\mu-\text{I})_4]\text{I}_3$. Systematic absences allowed the space groups $Cmcm$, $Cmc2_1$, and $C2cm$. Since only one of the two potential structural mirror planes is aligned with the crystallographic axes, either of the non-centrosymmetric alternatives was initially preferred. A chemically sensible and computationally stable structure was developed in $Cmc2_1$. The correctness of the reported enantiomorph was determined by the Rogers test.^{17c} Positional parameters are listed in Table 9, and selected bond distances and angles are collected in Table 10.

(f) $[\text{Cp}^*{}_{\text{2}}\text{Mo}_2(\mu-\text{Cl})_x(\mu-\text{I})_{4-x}]\text{I}_3$. The systematic absences in the diffraction data and the chemically sensible results of refinement established the space group as $Pn2_1a$. Attempted refinement under centrosymmetric $Pnma$ was much less satisfactory, resulting in physically unreasonable thermal and bond parameters for the metal and bridging halide atoms. The bridging halide atoms were found to be compositionally disordered, containing both I and Cl character. As a compromise, Br scattering factors were used. Individual atomic occupancies were then refined using common thermal parameters, and the percent I/Cl character for each bridging halide was calculated (% Cl, % I: ClI(1), 84.2, 15.8; ClI(2), 46.5, 53.5; ClI(3), 47.7, 52.3; ClI(4), 21.5, 78.5). Constraints were used to maintain a four-atom halogen stoichiometry. The carbon atoms were only refined isotropically, and the Cp^* rings were constrained as rigid groups. The correctness of the reported enantiomorph was determined by the Rogers test.^{17c} Positional parameters are listed in Table 11 and selected bond distances and angles are summarized in Table 10.

(g) $[\text{NMe}_3\text{Ph}][\text{Cp}^*\text{MoI}_4]$. The systematic absences in the diffraction data uniquely established the space group as monoclinic $P2_1/c$. The solution revealed two independent cations and two independent anions

Table 7. Positional and Isotropic Equivalent Thermal Parameters for $[\text{Cp}^*{}_{\text{2}}\text{Mo}_2\text{Br}_4]_2[\text{Cp}^*\text{MoBr}_4]_2\cdot 2\text{C}_7\text{H}_{16}$

atom	x	y	z	$U(\text{eq}), \text{\AA}^2$
Mo(1)	-0.021(4)	0.2500	0.4471(7)	0.079(6)
Mo(2)	-0.295(2)	0.0327(2)	-0.3453(3)	0.043(4)
Mo(3)	-0.3220(2)	-0.0397(2)	-0.1941(3)	0.043(4)
Mo(4)	0.3351(4)	0.2500	0.7005(5)	0.048(6)
Mo(5)	0.3324(4)	0.7500	-0.1226(5)	0.042(5)
Br(11)	-0.0579(7)	0.2500	0.6113(10)	0.139(14)
Br(12)	-0.0455(5)	0.3498(4)	0.4251(11)	0.181(13)
Br(13)	-0.0402(7)	0.2500	0.2386(11)	0.190(19)
Br(21)	-0.2889(4)	-0.0794(2)	-0.3786(5)	0.095(9)
Br(22)	-0.3353(4)	0.0733(2)	-0.1652(4)	0.074(7)
Br(23)	-0.4204(4)	-0.0071(3)	-0.3694(5)	0.094(6)
Br(24)	-0.1987(4)	0.0002(4)	-0.1685(6)	0.118(7)
Br(41)	0.2866(4)	0.3535(2)	0.6748(5)	0.080(6)
Br(42)	0.2923(5)	0.2500	0.4773(6)	0.072(8)
Br(43)	0.2756(5)	0.2500	0.8683(6)	0.071(8)
Br(51)	0.3708(4)	0.7500	0.1100(5)	0.050(6)
Br(52)	0.3782(3)	0.6459(2)	-0.0943(5)	0.077(5)
Br(53)	0.4058(5)	0.7500	-0.2744(7)	0.071(6)
C(11)	0.113(5)	0.250	0.405(5)	0.14(2)
C(12)	0.104(3)	0.2009(4)	0.468(3)	0.08(2)
C(13)	0.098(3)	0.220(1)	0.577(4)	0.10(2)
C(14)	0.139(6)	0.250	0.292(7)	0.18(3)
C(15)	0.118(5)	0.138(2)	0.437(5)	0.19(2)
C(16)	0.096(4)	0.183(2)	0.682(4)	0.10(2)
C(21)	-0.324(2)	0.070(2)	-0.525(4)	0.11(2)
C(22)	-0.257(2)	0.047(2)	-0.504(3)	0.05(1)
C(23)	-0.214(2)	0.079(2)	-0.414(3)	0.07(1)
C(24)	-0.254(2)	0.122(2)	-0.379(4)	0.08(2)
C(25)	-0.322(2)	0.117(2)	-0.450(4)	0.10(2)
C(26)	-0.386(4)	0.063(4)	-0.636(6)	0.28(3)
C(27)	-0.230(3)	0.005(3)	-0.582(5)	0.18(2)
C(28)	-0.134(2)	0.079(4)	-0.386(7)	0.24(3)
C(29)	-0.221(3)	0.170(3)	-0.291(6)	0.20(2)
C(30)	-0.384(4)	0.158(4)	-0.457(10)	0.45(3)
C(31)	-0.374(2)	-0.123(2)	-0.156(3)	0.07(1)
C(32)	-0.302(2)	-0.129(2)	-0.114(3)	0.06(1)
C(33)	-0.280(2)	-0.091(2)	-0.019(3)	0.06(1)
C(34)	-0.337(2)	-0.056(2)	-0.014(3)	0.05(1)
C(35)	-0.395(2)	-0.075(2)	-0.100(4)	0.09(2)
C(36)	-0.418(3)	-0.159(3)	-0.257(5)	0.16(2)
C(37)	-0.256(3)	-0.178(3)	-0.143(6)	0.18(2)
C(38)	-0.208(2)	-0.085(3)	0.059(4)	0.12(2)
C(39)	-0.342(3)	-0.014(3)	0.083(5)	0.15(2)
C(40)	-0.464(3)	-0.042(3)	-0.128(7)	0.24(3)
C(41)	0.431(5)	0.250	0.646(5)	0.11(2)
C(42)	0.420(5)	0.202(1)	0.711(5)	0.28(3)
C(43)	0.421(4)	0.222(2)	0.823(5)	0.16(2)
C(44)	0.453(6)	0.250	0.530(7)	0.16(3)
C(45)	0.443(7)	0.138(2)	0.691(8)	0.39(3)
C(46)	0.441(9)	0.179(4)	0.930(7)	0.60(3)
C(51)	0.232(5)	0.750	-0.088(5)	0.15(3)
C(52)	0.230(3)	0.798(1)	-0.161(4)	0.10(2)
C(53)	0.246(3)	0.778(2)	-0.262(4)	0.09(2)
C(54)	0.205(7)	0.750	0.023(7)	0.22(3)
C(55)	0.227(7)	0.863(2)	-0.131(7)	0.32(3)
C(56)	0.249(5)	0.816(3)	-0.369(5)	0.21(3)

^a Equivalent isotropic U defined as one-third of the trace of the orthogonalized U_{ij} tensor.

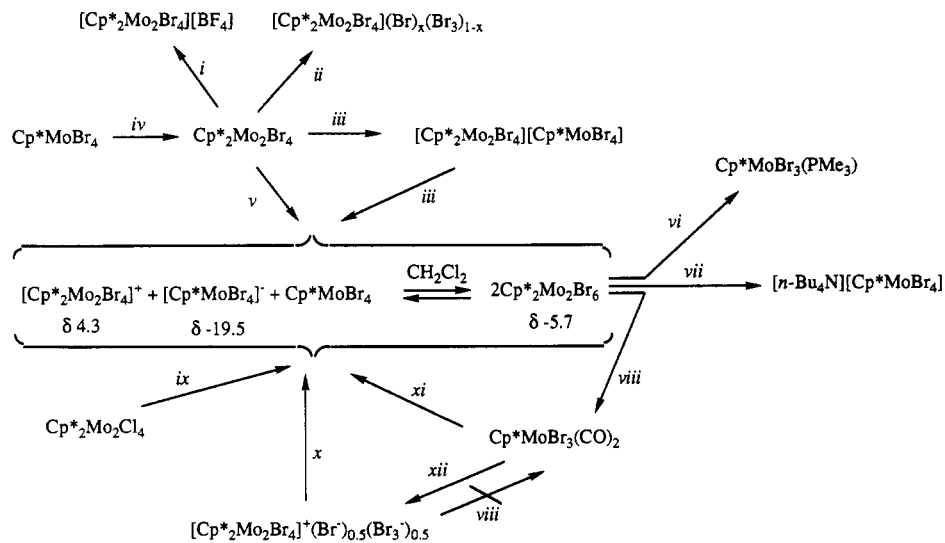
in the asymmetric unit. Positional parameters are listed in Table 12 and selected bond distances and angles are summarized in Table 13.

Results

Synthetic, Spectroscopic, Electrochemical, and Reactivity Studies. All the chemical transformations described in this contribution are summarized in Schemes 1 and 2.

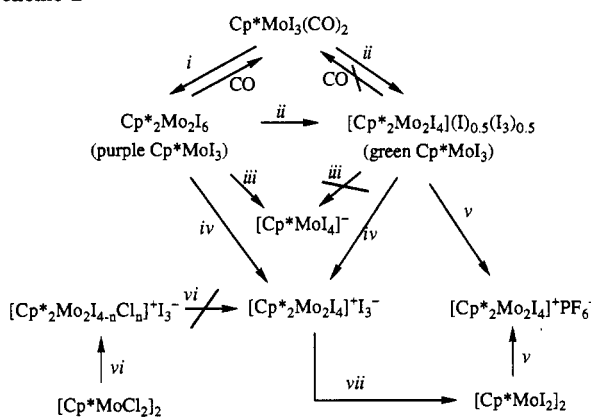
(a) Reduction of Cp^*MoBr_4 . Reduction of Cp^*MoBr_4 with 1 equiv of amalgamated sodium in toluene did not result in the formation of the expected tribromide compound but rather gave the previously unreported dibromide dimer, $\text{Cp}^*{}_{\text{2}}\text{Mo}_2\text{Br}_4$, leaving 50% of the starting material unreacted. The use of two reducing equivalents provided a high yield synthesis of the diamagnetic $\text{Cp}^*{}_{\text{2}}\text{Mo}_2\text{Br}_4$ whose crystal structure has been determined by

Scheme 1



i, AgBF₄ or NOBF₅/CH₂Cl₂; ii, Br₂/benzene; iii, Cp*MoBr₄ (1 equiv)/CH₂Cl₂; iv, Na(Hg)/toluene; v, Br₂/CH₂Cl₂, vi, PMe₃; vii, n-Bu₄NBr; viii, CO (1 atm); ix, HBr_(g)/CH₂Cl₂; x, CH₂Cl₂, r.t.; xi, Δ/CH₂Cl₂; xii, Δ/toluene

Scheme 2



i, Δ/CH₂Cl₂; ii, Δ/toluene; iii, I₂/CH₂Cl₂; iv, I₂/CH₂Cl₂; v, AgPF₆/CH₂Cl₂; vi, HI_(g)/CH₂Cl₂; vii, 1.5 equiv PMe₃/THF.

X-ray crystallography, and it is discussed later. The use of toluene as solvent is critical for this synthesis. When the same reaction was carried out in THF, no formation of the desired materials (either the tribromide compound when using 1 equiv of Na or the dibromide compound with 2 equiv) was observed by NMR. This contrasts with the reported reduction of (C₅H₄Me)MoBr₄ with Na/THF to afford (C₅H₄Me)₂Mo₂Br₄.^{2b} A reduction of the hypothetical Cp*MoI₄ complex could not be investigated because this compound is unknown and the studies that we have carried out (vide infra) prove that this would not be a stable compound.

(b) Decarbonylation of Cp*MoX₃(CO)₂. The precursor compounds have been obtained in a straightforward manner by oxidation of [Cp*Mo(CO)₃]₂ with the appropriate amount of the suitable dihalogen in CH₂Cl₂ and isolated in nearly quantitative yields. The analogous compounds CpMoX₃(CO)₂ (X = Cl, Br, I)¹⁸ and Cp*MoCl₃(CO)₂⁹ have been previously reported and Cp*MoI₃(CO)₂ has also been independently described¹⁴ while our studies were in progress. The CO stretching vibrations in the IR spectrum show the expected trend with lower wavenumbers on going from lighter to heavier halogen and on going from Cp to Cp*.

Table 8. Selected Bond Distances (Å) and Angles (deg) for {[Cp*₂Mo₂Br₄]⁺[Cp*MoBr₄]₂·Cp*MoBr₄·2C₇H₁₆}

(a) Bonds ^a			
Mo(1)-Br(11)	2.521(15)	Mo(3)-Br(23)	2.623(7)
Mo(1)-Br(12)	2.479(10)	Mo(3)-Br(24)	2.604(9)
Mo(1)-Br(13)	2.441(15)	Mo(3)-CNT(3)	1.96(5)
Mo(1)-CNT(1)	2.06(9)	Mo(4)-Br(41)	2.595(6)
Mo(2)-Mo(3)	2.643(5)	Mo(4)-Br(42)	2.616(9)
Mo(2)-Br(21)	2.655(7)	Mo(2)-Br(43)	2.609(11)
Mo(2)-Br(22)	2.682(7)	Mo(4)-CNT(4)	1.71(11)
Mo(2)-Br(23)	2.638(8)	Mo(5)-Br(51)	2.721(8)
Mo(2)-Br(24)	2.615(8)	Mo(5)-Br(52)	2.591(6)
Mo(2)-CNT(2)	1.95(6)	Mo(5)-Br(53)	2.639(10)
Mo(3)-Br(21)	2.653(7)	Mo(5)-CNT(5)	1.89(9)
Mo(3)-Br(22)	2.683(6)		
(b) Angles ^a			
Br(11)-Mo(1)-Br(12)	82.4(4)	Br(21)-Mo(3)-CNT(3)	118.6(9)
Br(11)-Mo(1)-Br(13)	136.6(6)	Br(22)-Mo(3)-Br(23)	74.9(2)
Br(11)-Mo(1)-CNT(1)	113.4(14)	Br(22)-Mo(3)-Br(24)	76.0(3)
Br(12)-Mo(1)-Br(13)	83.1(4)	Br(22)-Mo(3)-CNT(3)	120.9(9)
Br(12)-Mo(1)-Br(12A)	139.9(4)	Br(23)-Mo(3)-Br(24)	119.9(3)
Br(12)-Mo(1)-CNT(1)	110.0(3)	Br(23)-Mo(3)-CNT(3)	122.0(9)
Br(13)-Mo(1)-CNT(1)	110.0(14)	Br(24)-Mo(3)-CNT(3)	118.1(9)
Br(21)-Mo(2)-Br(22)	120.5(2)	Br(41)-Mo(4)-Br(22)	82.0(2)
Br(21)-Mo(2)-Br(23)	73.7(3)	Br(41)-Mo(4)-Br(43)	81.9(2)
Br(21)-Mo(2)-Br(24)	77.4(3)	Br(41)-Mo(4)-Br(41A)	137.0(2)
Br(21)-Mo(2)-CNT(2)	120.9(10)	Br(41)-Mo(4)-CNT(4)	111.5(20)
Br(22)-Mo(2)-Br(23)	74.7(3)	Br(42)-Mo(4)-Br(43)	134.9(4)
Br(22)-Mo(2)-Br(24)	75.9(3)	Br(42)-Mo(4)-CNT(4)	110.5(18)
Br(22)-Mo(2)-CNT(2)	118.8(10)	Br(43)-Mo(4)-CNT(4)	114.6(18)
Br(23)-Mo(2)-Br(24)	118.9(3)	Br(51)-Mo(5)-Br(53)	131.0(4)
Br(24)-Mo(2)-CNT(2)	120.2(10)	Br(51)-Mo(5)-CNT(5)	114.7(18)
Br(21)-Mo(3)-Br(22)	120.5(2)	Br(52)-Mo(5)-Br(53)	81.2(2)
Br(21)-Mo(3)-Br(23)	74.0(3)	Br(52)-Mo(5)-Br(52A)	139.3(2)
Br(21)-Mo(3)-Br(24)	77.7(3)	Br(52)-Mo(5)-CNT(5)	110.4(20)
Br(53)-Mo(5)-CNT(5)	114.3(17)		

^a CNT = centroid of the Cp* ring.

The decarbonylation of Cp*MoX₃(CO)₂ (X = Br, I) in either refluxing dichloromethane or toluene leads to complete loss of all CO stretchings from the solutions. The nature of the resulting product(s) depends, however, on the conditions employed. From the iodide compound in refluxing CH₂Cl₂, a single purple product, slightly soluble in aromatic hydrocarbons and very soluble in CH₂Cl₂, is obtained. This product shows a paramagnetically shifted ¹H-NMR resonance at δ = 5.1 in CD₂Cl₂ and corresponds to the molecular dinuclear species Cp*₂Mo₂(μ-I)₂I₄. The

(18) (a) Haines, R. J.; Nyholm, R. S.; Stiddard, M. H. B. *J. Chem. Soc. A* 1966, 1606. (b) Green, M. L. H.; Lindsell, W. E. *J. Chem. Soc. A* 1967, 686.

Table 9. Atomic Coordinates ($\times 10^4$) and Isotropic Thermal Parameters ($\text{\AA}^2 \times 10^3$) for $[\text{Cp}^*{}_{\text{2}}\text{Mo}_2\text{I}_4]\text{I}_3$

atom	x	y	z	U^a
Mo(1)	10000	2924(2)	7616	20(1)
Mo(2)	10000	4243(2)	8676(2)	20(1)
I(1)	10000	4844(1)	7248(2)	35(1)
I(2)	10000	2329(1)	9029(2)	37(1)
I(3)	7930(1)	3582(1)	8138(2)	36(1)
I(4)	10000	2068(2)	11733(3)	54(1)
I(5)	10000	512(2)	10704(2)	45(1)
I(6)	10000	-1005(2)	9652(3)	62(1)
C(1)	10000	1277(17)	7259(18)	22(9)
C(2)	9004(21)	1758(12)	6951(15)	35(8)
C(3)	9444(22)	2463(13)	6504(11)	32(7)
C(4)	10000	477(23)	7730(24)	54(16)
C(5)	7859(20)	1375(14)	7062(16)	42(8)
C(6)	8545(29)	3034(19)	5980(15)	64(12)
C(7)	10000	5856(20)	9037(20)	33(8)
C(8)	9028(19)	5445(13)	9330(12)	27(6)
C(9)	9369(21)	4658(12)	9780(12)	27(7)
C(10)	10000	6744(19)	8532(19)	40(13)
C(11)	7743(25)	5703(19)	9246(18)	60(11)
C(12)	8624(23)	4112(16)	10248(14)	40(8)

^a Equivalent isotropic U defined as one-third of the trace of the orthogonalized U_{ij} tensor.

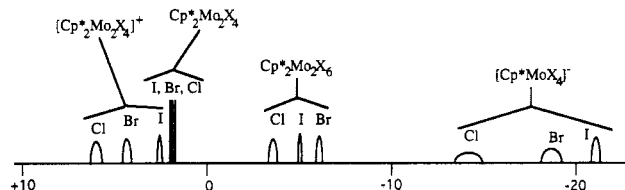


Figure 1. Approximate position and line width for the ^1H -NMR resonances of all Cp^* species described in this paper. For comparison, the resonances of the previously reported⁹ analogous Cl complexes are also shown.

structural assignment is based on the comparison of the chemical shift with that of the analogous chloride compound (δ -4.2 in CD_2Cl_2), for which an X-ray structure was determined and found to be consistent with the solid state and solution magnetic properties.⁹ In addition, the reactivity of this purple material is identical with that of the other $\text{Cp}^*{}_{\text{2}}\text{Mo}_2\text{X}_6$ ($\text{X} = \text{Cl}, \text{Br}$) analogues and, most importantly, different from that of other forms of “ CpMoX_3 ” ($\text{X} = \text{Br}, \text{I}$), as will be shown later. For convenience, the ^1H -NMR resonances of all the Cp^* species discussed in this paper are qualitatively illustrated in Figure 1. Most of the chemistry discussed in this contribution has been elucidated with the help of ^1H -NMR, which turned out to be a formidable source of information even though most of the species investigated are paramagnetic.

Decarbonylation of the bromide compound in CH_2Cl_2 is more complex with respect to that of the iodide analogue. The isolated solid has a resonance at δ -5.7 in CDCl_3 due to $[\text{Cp}^*{}_{\text{2}}\text{Mo}_2(\mu\text{-Br})_2\text{Br}_4]$ and resonances at δ 4.5 and -19.5 due to $[\text{Cp}^*{}_{\text{2}}\text{Mo}_2\text{Br}_4]^+$ and $[\text{Cp}^*\text{MoBr}_4]^-$, respectively. The assignment of these ^1H -NMR resonances is confirmed by the independent syntheses of all of the above complexes (vide infra). Due to oxidation state balance, the presence of the Mo(V) complex Cp^*MoBr_4 , for which the ^1H -NMR resonance is too broad to be observed, is also inferred. This is confirmed by the reaction with neutral donors to give only complexes of Mo(IV) as products and by the alternative preparation of the same mixture of compounds by conproportionation of $\text{Cp}^*{}_{\text{2}}\text{Mo}_2\text{Br}_4$ and Cp^*MoBr_4 , as shown later.

The decarbonylation of both $\text{Cp}^*\text{MoX}_3(\text{CO})_2$ ($\text{X} = \text{Br}, \text{I}$) compounds under more forcing conditions (refluxing toluene) results instead in the formation of products that are insoluble in toluene and soluble in CH_2Cl_2 . These materials exhibit only the resonance of the $[\text{Cp}^*{}_{\text{2}}\text{Mo}_2\text{X}_4]^+$ ion in the ^1H -NMR spectrum (CD_2Cl_2). Since these species analyze correctly for Cp^*MoX_3 , the oxidation state balance demands that the counterion for $[\text{Cp}^*{}_{\text{2}}$

Table 10. Selected Bond Distances (\AA) and Angles (deg) for $\{[\text{Cp}^*\text{Mo}(\mu\text{-Cl})_{x}(\mu\text{-I})_{2-x}]_2\}\text{I}_3$ ($x = 0, 1$)^a

	$\{[\text{Cp}^*\text{MoI}_2]_2\}\text{I}_3$	$\{[\text{Cp}^*\text{MoCl}]_2\}\text{I}_3$	
(a) Distances ^b			
Mo(1)-Mo(2)	2.718(3)	Mo(1)-Mo(2)	2.658(2)
Mo(1)-I(1)	2.793(3)	Mo(1)-ICl(1)	2.671(4)
Mo(1)-I(2)	2.772(4)	Mo(1)-ICl(2)	2.784(5)
Mo(1)-I(3)	2.782(2)	Mo(1)-ICl(3)	2.729(5)
		Mo(1)-ICl(4)	2.769(2)
Mo(2)-I(1)	2.799(5)	Mo(2)-ICl(1)	2.674(4)
Mo(2)-I(2)	2.780(3)	Mo(2)-ICl(2)	2.747(7)
Mo(2)-I(3)	2.793(2)	Mo(2)-ICl(3)	2.751(8)
		Mo(2)-ICl(4)	2.776(2)
Mo(1)-CNT(1)	2.012(6)	Mo(1)-CNT(1)	1.98(1)
Mo(2)-CNT(2)	1.993(6)	Mo(2)-CNT(2)	1.97(1)
I(4)-I(5)	2.919(5)	I(5)-I(6)	2.922(2)
I(5)-I(6)	2.906(5)	I(6)-I(7)	2.908(3)
(b) Angles ^b			
I(1)-Mo(1)-I(2)	121.9(1)	CII(1)-Mo(1)-CII(4)	121.7(1)
I(3)-Mo(1)-Mo(3a)	122.1(1)	CII(2)-Mo(1)-CII(3)	122.0(2)
I(1)-Mo(2)-I(2)	121.3(1)	CII(1)-Mo(2)-CII(4)	121.3(1)
I(3)-Mo(2)-Mo(3a)	121.2(2)	CII(2)-Mo(2)-CII(3)	122.6(2)
I(1)-Mo(1)-I(3)	76.3(1)	CII(1)-Mo(1)-CII(2)	75.9(3)
I(2)-Mo(1)-I(3)	76.5(1)	CII(1)-Mo(1)-CII(3)	76.5(3)
		CII(2)-Mo(1)-CII(4)	76.0(2)
		CII(3)-Mo(1)-CII(4)	77.0(2)
I(1)-Mo(2)-I(3)	76.0(1)	CII(1)-Mo(2)-CII(2)	76.5(3)
I(2)-Mo(2)-I(3)	76.2(1)	CII(1)-Mo(2)-CII(3)	76.1(3)
		CII(2)-Mo(2)-CII(4)	76.5(2)
		CII(3)-Mo(2)-CII(4)	76.5(2)
Mo(2)-Mo(1)-CNT(1)	179.8(6)	Mo(2)-Mo(1)-CNT(1)	176.5(3)
Mo(1)-Mo(2)-CNT(2)	179.9(6)	Mo(1)-Mo(2)-CNT(2)	176.3(5)
I(1)-Mo(1)-CNT(1)	119.2(6)	CII(1)-Mo(1)-CNT(1)	116.7(3)
I(2)-Mo(1)-CNT(1)	119.0(6)	CII(2)-Mo(1)-CNT(1)	121.0(5)
I(3)-Mo(1)-CNT(1)	119.0(6)	CII(3)-Mo(1)-CNT(1)	117.0(5)
		CII(4)-Mo(1)-CNT(1)	121.6(3)
I(1)-Mo(2)-CNT(2)	119.1(5)	CII(1)-Mo(2)-CNT(2)	117.2(3)
I(2)-Mo(2)-CNT(2)	119.6(5)	CII(2)-Mo(2)-CNT(2)	115.5(5)
I(3)-Mo(2)-CNT(2)	119.4(6)	CII(3)-Mo(2)-CNT(2)	121.9(5)
		CII(4)-Mo(2)-CNT(2)	121.4(3)
Mo(1)-I(1)-Mo(2)	58.2(1)	Mo(1)-CII(1)-Mo(2)	59.7(1)
Mo(1)-I(2)-Mo(2)	58.6(1)	Mo(1)-CII(2)-Mo(2)	57.4(1)
Mo(1)-I(3)-Mo(2)	58.4(1)	Mo(1)-CII(3)-Mo(2)	58.0(1)
		Mo(1)-CII(4)-Mo(2)	57.3(1)
I(4)-I(5)-I(6)	178.7(2)	I(5)-I(6)-I(7)	179.1(1)

^a On each section of the table, equivalent parameters for the two different molecules are compared side-by-side. ^b CNT = centroid of the Cp^* ring.

$\text{Mo}_2\text{X}_4]^+$ is “ X_2^- ”, which must therefore correspond to a 1:1 mixture of X_2^- and X_3^- . In this respect, it is worth pointing out a certain analogy with the structure of Cp^*CrI_3 , which corresponds in fact to a polymeric chain of formula $\{[\text{Cp}^*\text{Cr}_2(\mu\text{-I})_2\text{I}_2][\text{Cp}^*\text{Cr}_2(\mu\text{-I})_2(\text{I}_3)_2]\}^{11}$. When $\text{Cp}^*\text{MoBr}_3(\text{CO})_2$ is decarbonylated in refluxing toluene for only a short time, the resonance of $\text{Cp}^*\text{Mo}_2\text{Br}_6$ is also evident in the isolated product, indicating that the molecular Mo(IV) dimer is the first product of the decarbonylation and this is then transformed to the $[\text{Cp}^*\text{Mo}_2\text{Br}_4]^+(\text{Br}^-)_{0.5}(\text{Br}_3^-)_{0.5}$ material under prolonged reflux. $\text{Cp}^*\text{Mo}_2\text{I}_6$, i.e. the purple product from the decarbonylation of $\text{Cp}^*\text{MoI}_3(\text{CO})_2$ in CH_2Cl_2 , analogously transforms into green $[\text{Cp}^*\text{Mo}_2\text{I}_4]^+(\text{I}^-)_{0.5}(\text{I}_3^-)_{0.5}$ when refluxed in toluene. The nonpolar characteristics of the solvent probably aid in this transformation. This is suggested by the behavior of $[\text{Cp}^*\text{Mo}_2\text{Br}_4]^+(\text{Br}^-)_{0.5}(\text{Br}_3^-)_{0.5}$ upon dissolution in CH_2Cl_2 . While only the ^1H -NMR resonance of the $[\text{Cp}^*\text{Mo}_2\text{Br}_4]^+$ ion is observed initially, the resonances of $\text{Cp}_2\text{Mo}_2\text{Br}_6$ and $[\text{Cp}^*\text{MoBr}_4]^-$ subsequently appear, therefore the transformation to the same mixture obtained by decarbonylation of $\text{Cp}^*\text{MoBr}_3(\text{CO})_2$ in CH_2Cl_2 (Scheme 1) is suggested. On the other hand, dissolution of $[\text{Cp}^*\text{Mo}_2\text{I}_4]^+(\text{I}^-)_{0.5}(\text{I}_3^-)_{0.5}$ in CH_2Cl_2

Table 11. Atomic Coordinates ($\times 10^4$) and Equivalent Isotropic Displacement Coefficients ($\text{\AA} \times 10^3$) for $[\text{Cp}^*{}_{\text{2}}\text{Mo}_2\text{Cl}_{4-x}\text{I}_{4-x}]_3$

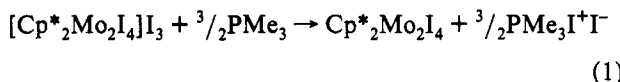
atom	x	y	z	U^a
Mo(1)	5765(1)	7500	3315(1)	37(1)
Mo(2)	6565(1)	7499(5)	5005(1)	40(1)
CII(1)	6951(2)	7479(13)	2852(3)	75(1)
CII(2)	6185(3)	9539(4)	4172(6)	64(1)
CII(3)	6145(3)	5485(4)	4167(6)	69(1)
CII(4)	5337(1)	7542(6)	5526(1)	58(1)
I(5)	2851(1)	7491(6)	5371(2)	79(1)
I(6)	3709(1)	7493(5)	7263(1)	63(1)
I(7)	4548(1)	7504(6)	9170(2)	80(1)
C(1)	5571(4)	6825(17)	1571(8)	42(4)
C(2)	5571	8016	1485	51(4)
C(3)	5067	8430	2108	81(4)
C(4)	4755	7495	2580	49(3)
C(5)	5067	6503	2248	24(3)
C(6)	5916(22)	6182(32)	722(30)	111(4)
C(7)	5971(12)	8878(20)	904(18)	36(3)
C(8)	4831(18)	9695(28)	2137(26)	77(4)
C(9)	4145(10)	7315(26)	3187(19)	66(4)
C(10)	4881(14)	5385(23)	2418(21)	48(4)
C(11)	7053(5)	6628(17)	6494(9)	47(4)
C(12)	6817	7641	6954	44(3)
C(13)	7093	8555	6374	73(4)
C(14)	7500	8106	5556	40(4)
C(15)	7475	6915	5630	56(4)
C(16)	6897(14)	5370(24)	6859(25)	64(4)
C(17)	6388(11)	7755(23)	7949(20)	67(4)
C(18)	7094(17)	9768(29)	6743(31)	101(4)
C(19)	7808(17)	9088(31)	4877(27)	100(4)
C(20)	7925(11)	6209(20)	4972(19)	42(4)

^a Equivalent isotropic U defined as one-third of the trace of the orthogonalized U_{ij} tensor.

generates a stable green solution, and no formation of $\text{Cp}^*{}_{\text{2}}\text{Mo}_2\text{I}_6$ occurs over several days.

The interaction of $[\text{Cp}^*{}_{\text{2}}\text{Mo}_2\text{I}_4]^+(\text{I}^-)_{0.5}(\text{I}_3^-)_{0.5}$ with $1/2$ equiv of I_2 resulted in the formation of the salt $[\text{Cp}^*{}_{\text{2}}\text{Mo}_2\text{I}_4]^+\text{I}_3^-$, which has the same emerald green color of its "green Cp^*Mol_3 " precursor and shows the same $^1\text{H-NMR}$ resonance assigned to the Cp^* protons of the cation. The given formulation for this triiodide salt is confirmed by cyclic voltammetric data and by an X-ray structural determination, both of which will be discussed later.

(c) **Electrochemical and Chemical Oxidation of $\text{Cp}^*{}_{\text{2}}\text{Mo}_2\text{X}_4$ and Characterization of $[\text{Cp}^*{}_{\text{2}}\text{Mo}_2\text{X}_4]^+$ Salts.** As mentioned above, the Mo(III) bromide compound, $\text{Cp}^*{}_{\text{2}}\text{Mo}_2\text{Br}_4$ was obtained by direct reduction of Cp^*MoBr_4 . The corresponding iodide system has eventually been obtained by reduction of the $[\text{Cp}^*{}_{\text{2}}\text{Mo}_2\text{I}_4]\text{I}_3$ after unsuccessful attempts to carry out a halide exchange from $\text{Cp}^*{}_{\text{2}}\text{Mo}_2\text{Cl}_4$, the unexpected result of which is illustrated later. We learned that "green Cp^*Mol_3 ", first reported by us,¹³ can be conveniently reduced to $\text{Cp}^*{}_{\text{2}}\text{Mo}_2\text{I}_4$ by reaction with 1 equiv of PMo_3 , the other product being presumably $\text{PMo}_3\text{I}^+\text{I}^-$.¹⁶ We have subsequently found that an analogous reduction can be carried out on the triiodide salt by properly adjusting the PMo_3 stoichiometry (eq 1), in further accord with the given formulation for "green Cp^*Mol_3 ".



The $\text{Cp}^*{}_{\text{2}}\text{Mo}_2\text{X}_4$ ($\text{X} = \text{Br}, \text{I}$) compounds show a single sharp Cp^* resonance (δ 2.11 for $\text{X} = \text{I}$ and 1.93 for $\text{X} = \text{Br}$ in CDCl_3 , compared with 1.84 for the previously reported⁹ compound with $\text{X} = \text{Cl}$). These NMR spectra indicate the diamagnetism of these materials, which is consistent with their solid-state structure. The structure of the similar $(\text{C}_5\text{H}_4\text{-i-Pr})_2\text{Mo}_2\text{Cl}_4$,^{2a} $(\text{C}_5\text{Me}_4\text{-Et})_2\text{Mo}_2\text{Cl}_4$,¹⁹ and $\text{Cp}^*{}_{\text{2}}\text{Mo}_2\text{Br}_4$ ($\text{Cp}^* = \text{C}_5\text{Ph}_5[2,5\text{-C}_6\text{H}_3\text{-}(\text{OMe})_2]$)²⁰ compounds has been determined and found to be

Table 12. Atomic Coordinates ($\times 10^4$) and Equivalent Isotropic Displacement Coefficients ($\text{\AA} \times 10^3$) for $[\text{NMe}_2\text{Ph}][\text{Cp}^*\text{Mol}_3]$

atom	x	y	z	$B(\text{eq})$
I(11)	0.7355(2)	0.1807(1)	0.44152(9)	5.8(1)
I(12)	0.4565(2)	0.3212(1)	0.44616(8)	5.3(1)
I(13)	0.9950(2)	0.3166(1)	0.41418(9)	5.3(1)
I(14)	0.7231(2)	0.4593(1)	0.41852(8)	5.0(1)
I(21)	0.5133(2)	0.3129(1)	0.08135(8)	4.8(1)
I(22)	0.5151(2)	0.2957(1)	0.20428(8)	5.4(1)
I(23)	0.2401(2)	0.4554(1)	0.08597(8)	5.1(1)
I(24)	0.2320(3)	0.4301(1)	0.2044(1)	7.0(1)
Mo(1)	0.69216	0.3119(1)	0.39511	2.9(1)
Mo(2)	0.2937(2)	0.3312(1)	0.1386(1)	3.3(1)
N(1)	0.251(2)	0.058(1)	0.4341(8)	4(1)
N(2)	0.778(3)	0.067(1)	0.067(1)	5(1)
C(1)	0.720(3)	0.338(2)	0.320(1)	4.9(7)
C(2)	0.736(3)	0.264(2)	0.327(1)	4.4(7)
C(3)	0.608(3)	0.237(2)	0.333(1)	5.3(8)
C(4)	0.512(4)	0.294(2)	0.337(1)	5.9(8)
C(5)	0.573(5)	0.356(3)	0.329(2)	9(1)
C(6)	0.087(3)	0.277(2)	0.095(1)	4.6(7)
C(7)	0.044(3)	0.296(2)	0.135(1)	5.3(8)
C(8)	0.139(3)	0.248(2)	0.168(1)	5.3(8)
C(9)	0.227(3)	0.206(2)	0.144(1)	4.7(7)
C(10)	0.191(3)	0.226(2)	0.099(1)	5.4(8)
C(11)	0.833(6)	0.387(3)	0.303(2)	14(2)
C(21)	0.853(7)	0.215(4)	0.313(3)	19(2)
C(31)	0.554(7)	0.162(4)	0.336(3)	19(3)
C(41)	0.341(7)	0.291(4)	0.337(2)	17(2)
C(51)	0.519(6)	0.439(3)	0.316(2)	15(2)
C(61)	0.001(4)	0.314(2)	0.056(2)	10(1)
C(71)	-0.072(4)	0.344(2)	0.150(2)	9(1)
C(81)	0.118(4)	0.242(2)	0.214(2)	9(1)
C(91)	0.319(4)	0.144(2)	0.158(2)	10(1)
C(101)	0.249(5)	0.187(3)	0.058(2)	12(2)
C(300)	0.237(6)	-0.014(4)	0.456(2)	15(2)
C(301)	0.136(8)	0.094(4)	0.454(3)	19(3)
C(302)	0.382(7)	0.085(3)	0.455(2)	15(2)
C(303)	0.239(3)	0.050(2)	0.385(1)	4.3(7)
C(304)	0.341(3)	0.010(2)	0.367(1)	4.2(6)
C(305)	0.133(5)	0.077(2)	0.312(2)	9(1)
C(306)	0.230(3)	0.036(2)	0.293(1)	5.7(8)
C(307)	0.326(4)	0.004(2)	0.318(1)	8(1)
C(308)	0.138(4)	0.086(2)	0.362(1)	7(1)
C(400)	0.844(8)	0.005(4)	0.048(3)	19(2)
C(401)	0.813(7)	0.139(4)	0.046(3)	19(3)
C(402)	0.622(6)	0.057(3)	0.051(2)	14(2)
C(403)	0.798(3)	0.072(2)	0.117(1)	4.5(7)
C(404)	0.744(4)	0.131(2)	0.137(1)	7(1)
C(405)	0.756(4)	0.125(2)	0.184(2)	8(1)
C(406)	0.821(4)	0.077(2)	0.210(1)	7(1)
C(407)	0.875(3)	0.018(2)	0.185(1)	6.1(8)
C(408)	0.862(4)	0.018(2)	0.140(1)	8(1)

dinuclear with four halide ligands bridging the two metal atoms which are also directly bonded to each other to give a formal 18-electron count to each metal. We have determined the structure of $\text{Cp}^*{}_{\text{2}}\text{Mo}_2\text{Br}_4$, which is found to be also of the quadruply-bridged type (vide infra), and Parkin has also found the same structural motif in $\text{Cp}^*{}_{\text{2}}\text{Mo}_2\text{I}_4$.^{16b}

The $\text{Cp}^*{}_{\text{2}}\text{Mo}_2\text{X}_4$ ($\text{X} = \text{Br}, \text{I}$) compounds exhibit two reversible oxidation processes in the cyclic voltammogram. The half-wave potentials are shown pictorially in Figure 2, together with those of the analogous chloro compound and of the other species investigated electrochemically during the course of this study. The half-wave potentials for the $\text{Cp}^*{}_{\text{2}}\text{Mo}_2\text{X}_4/[\text{Cp}^*{}_{\text{2}}\text{Mo}_2\text{X}_4]^+$ and $[\text{Cp}^*{}_{\text{2}}\text{Mo}_2\text{X}_4]^+/\text{Cp}^*{}_{\text{2}}\text{Mo}_2\text{X}_4^{2+}$ couples are little dependent on the nature of the halide (see Figure 2). The products of one-electron oxidation were obtained and isolated in good yields by interaction of $\text{Cp}^*{}_{\text{2}}\text{Mo}_2\text{X}_4$ with AgBF_4 or NOBF_4 (for $\text{X} = \text{Br}$) and with AgPF_6 (for $\text{X} = \text{I}$), resulting in the precipitation of metallic Ag or evolution of gaseous NO. The color of these salts is red for $\text{X} = \text{Br}$ and dark emerald green for $\text{X} = \text{I}$, the latter

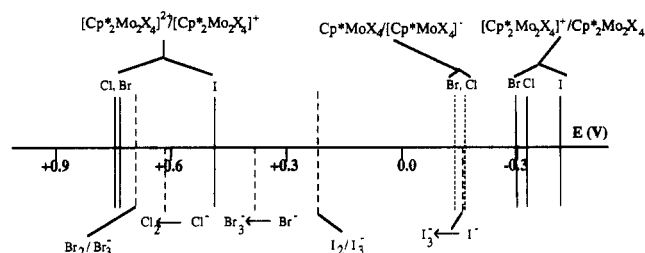


Figure 2. Approximate positions on the potential scale of the redox processes investigated during this study. For comparison, the redox processes of the previously reported⁹ analogous Cl complexes are also shown. Bars extending above and below the potential axis indicate electrochemically reversible processes; bars that extend only below the potential axis are located at the anodic peak potential of irreversible oxidation processes. Potentials are with respect to the $\text{Cp}_2\text{Fe}/\text{Cp}_2\text{Fe}^+$ $E_{1/2}$ value.

Table 13. Selected Bond Distances (\AA) and Angles (deg) for $[\text{NMe}_3\text{Ph}][\text{Cp}^*\text{MoI}_4]$

(a) Distances			
Mo(1)-I(11)	2.802(3)	Mo(1)-I(12)	2.785(2)
Mo(1)-I(13)	2.814(2)	Mo(1)-I(14)	2.817(4)
Mo(2)-I(21)	2.799(3)	Mo(2)-I(22)	2.786(3)
Mo(2)-I(23)	2.800(4)	Mo(2)-I(24)	2.784(4)
Mo(1)-CNT(1)	2.02(5)	Mo(2)-CNT(2)	2.08(3)

(b) Angles			
I(11)-Mo(1)-I(2)	82.26(8)	I(11)-Mo(1)-I(13)	80.31(7)
I(11)-Mo(1)-I(14)	134.77(8)	I(12)-Mo(1)-I(13)	134.84(7)
I(12)-Mo(1)-I(14)	82.57(8)	I(13)-Mo(1)-I(14)	80.94(8)
CNT(1)-Mo(1)-I(11)	113(1)	CNT(1)-Mo(1)-I(12)	112(1)
CNT(1)-Mo(1)-I(13)	113(1)	CNT(1)-Mo(1)-I(14)	112(1)
I(21)-Mo(2)-I(22)	82.8(1)	I(21)-Mo(2)-I(23)	81.7(1)
I(21)-Mo(2)-I(24)	136.1(1)	I(22)-Mo(2)-I(23)	132.1(1)
I(22)-Mo(2)-I(24)	80.8(1)	I(23)-Mo(2)-I(24)	79.8(1)
CNT(2)-Mo(2)-I(21)	110(1)	CNT(2)-Mo(2)-I(22)	113(1)
CNT(2)-Mo(2)-I(23)	115(1)	CNT(2)-Mo(2)-I(24)	113(1)

color being identical to that observed for the triiodide salt and for "green Cp^*MoI_3 ". $[\text{Cp}^*\text{Mo}_2\text{I}_4]^+\text{PF}_6^-$ also forms by ion metathesis from $[\text{Cp}^*\text{Mo}_2\text{I}_4]^+(\text{I}^-)_{0.5}(\text{I}_3^-)_{0.5}$ and AgPF_6 , the byproducts being presumably insoluble AgI and AgI_3 . These products show the expected one-electron reduction and one-electron oxidation in the cyclic voltammogram at the same potentials observed for the two oxidation processes of the parent Mo(III) compounds and their $^1\text{H-NMR}$ properties are as discussed above and as illustrated in Figure 1.

The second oxidation process (that relating Mo_2^{7+} and Mo_2^{8+} species) is chemically reversible on the CV time scale (scan speeds as slow as 50 mV s^{-1}) for $\text{X} = \text{Br}$ and I , whereas the return reduction wave has decreased intensity at slow scan speeds for $\text{X} = \text{Cl}$.⁹ However, the dicationic complex does not appear to be stable when generated by chemical oxidation. Treatment of $[\text{Cp}^*\text{Mo}_2\text{I}_4]^+\text{PF}_6^-$ with a second equivalent of AgPF_6 leads to precipitation of a gray solid, probably metallic silver, but unexpectedly, the color and the $^1\text{H-NMR}$ properties of the solution do not change. Subsequent treatment with additional AgPF_6 affords more gray precipitate, but again there is no evidence for change in the molybdenum complex. This process was not investigated further.

As illustrated above, the triiodide salt of $[\text{Cp}^*\text{Mo}_2\text{I}_4]^+$ was obtained by treatment of $[\text{Cp}^*\text{Mo}_2\text{I}_4]^+(\text{I}^-)_{0.5}(\text{I}_3^-)_{0.5}$ with the proper amount of I_2 . The same product was also obtained by interaction of I_2 with $\text{Cp}^*\text{Mo}_2\text{I}_6$. The cyclic voltammetric properties of this compound (described in detail in our preliminary communication)¹³ show the oxidation and reduction waves due to the cation, plus the electrochemical processes attributable to the I_3^- counterion (reversible oxidation to I_2 and irreversible reduction to I^-). The latter redox processes are also included in Figure 2. The fact that the I_3^- ion does not have sufficient oxidizing power to convert the $[\text{Cp}^*\text{Mo}_2\text{I}_4]^+$ ion to the corresponding

dication is evident in Figure 2 and rationalizes the redox stability of the triiodide salt.

The oxidation of $\text{Cp}^*\text{Mo}_2\text{Br}_4$ with Br_2 was also investigated. The result of this reaction is highly dependent on the nature of the solvent. When the reaction is carried out in a nonpolar solvent (benzene), a red precipitate is immediately obtained. This material shows only the NMR properties due to the $[\text{Cp}^*\text{Mo}_2\text{Br}_4]^+$ ion, and its elemental analysis shows a lower C and H content than expected for " Cp^*MoBr_3 ", the formulation best approaching the experimental values being $\text{Cp}^*\text{MoBr}_{3.3}$. The compound is therefore interpreted as a $[\text{Cp}^*\text{Mo}_2\text{Br}_4]^+(\text{Br}^-)_x(\text{Br}_3^-)_{1-x}$ material, with x ca. 0.2. The precipitation of the product immediately upon addition of Br_2 makes a better control of the stoichiometry impossible. Dissolution of this material in CH_2Cl_2 produces the same changes in the $^1\text{H-NMR}$ spectrum that are observed when dissolving $[\text{Cp}^*\text{Mo}_2\text{Br}_4]^+(\text{Br}^-)_{0.5}(\text{Br}_3^-)_{0.5}$, the product of thermal decarbonylation of $\text{Cp}^*\text{MoBr}_3(\text{CO})_2$ in refluxing toluene (vide supra); i.e., a mixture of the species that participate to the equilibrium shown in Scheme 1 is slowly formed. From a CH_2Cl_2 /heptane recrystallization of this material, single crystals of $[(\text{Cp}^*\text{Mo}_2\text{Br}_4)^+(\text{Cp}^*\text{MoBr}_3\cdot 2\text{C}_7\text{H}_{16})]$ have been obtained.¹²

The formulation of the $[\text{Cp}^*\text{Mo}_2\text{Br}_4]^+(\text{Br}^-)_x(\text{Br}_3^-)_{1-x}$ material is consistent with the cyclic voltammogram recorded on a *fresh* solution of the compound, which exhibits the reversible oxidation and reduction waves of the $[\text{Cp}^*\text{Mo}_2\text{Br}_4]^+$ ion, in addition to the redox processes of the $\text{Br}^-/\text{Br}_3^-/\text{Br}_2$ systems as verified by a control CV experiment on a bromide salt. These processes are also illustrated qualitatively in Figure 2 (E_{pa} for the irreversible oxidation of Br^- to Br_3^- at +0.38 V and $E_{1/2}$ for the quasi-reversible $\text{Br}_3^-/\text{Br}_2$ couple at +0.67 V). These numbers compare favorably with the literature values of 0.750 and 1.060 V vs SCE, respectively,²¹ considering the reported shift of $\text{Cp}_2\text{Fe}/\text{Cp}_2\text{Fe}^+$ vs SCE of +0.307 V in MeCN/0.2M LiClO₄²² and the expected solvent dependency.

The bromine oxidation of $\text{Cp}^*\text{Mo}_2\text{Br}_4$ in CH_2Cl_2 produces directly the mixture of compounds (Scheme 1) obtained also by dissolving $[\text{Cp}^*\text{Mo}_2\text{Br}_4]^+(\text{Br}^-)_x(\text{Br}_3^-)_{1-x}$, or thermally decarbonylating $\text{Cp}^*\text{MoBr}_3(\text{CO})_2$ in CH_2Cl_2 . Crystallization of this mixture from $1,1,2-\text{C}_2\text{H}_3\text{Cl}_3/\text{C}_6\text{H}_6$ produced single crystals of $\text{Cp}^*\text{Mo}_2\text{Br}_6\cdot \text{C}_6\text{H}_6$, which show the $^1\text{H-NMR}$ resonance reported in Figure 1. Taken together, all these experiments show that the initial step in the dibromine oxidation of $\text{Cp}^*\text{Mo}_2\text{Br}_4$ is electron transfer to the mixed-valence Mo(III,IV) cation and a mixture of Br^- and Br_3^- , as predicted by a comparison of the redox potentials in Figure 2. Br_2 and Br_3^- do not have sufficient power to oxidize the Mo complex any further, and therefore the $[\text{Cp}^*\text{Mo}_2\text{Br}_4]^+(\text{Br}^-)_x(\text{Br}_3^-)_{1-x}$ salt precipitates directly in a nonpolar solvent or rearranges further in CH_2Cl_2 according to a mechanism that will be discussed in detail in the Discussion section. It is relevant to note that an analogous dibromine oxidation of the aforementioned $\text{Cp}^*\text{Mo}_2\text{Br}_4$ compound has been reported²⁰ to produce the corresponding $[\text{Cp}^*\text{Mo}_2\text{Br}_4]^+\text{Br}_3^-$ salt, whose cyclic voltammetric properties are similar to those observed by us for our $[\text{Cp}^*\text{Mo}_2\text{Br}_4]^+(\text{Br}^-)_x(\text{Br}_3^-)_{1-x}$ compound. However, the chemistry of $[\text{Cp}^*\text{Mo}_2\text{Br}_4]^+\text{Br}_3^-$ does not appear to be complicated by subsequent rearrangement reactions, which undoubtedly was key to the isolation by Colbran and coworkers of the pure tribromide compound from a CH_2Cl_2 solution.²⁰

The salt $[\text{Cp}^*\text{Mo}_2\text{Br}_4]^+\text{BF}_4^-$ reacts slowly with Br^- ions to afford $[\text{Cp}^*\text{MoBr}_4]^-$ as the only observable new species by $^1\text{H-NMR}$. On the other hand, the analogous $[\text{Cp}^*\text{Mo}_2\text{I}_4]^+\text{PF}_6^-$ salt does not show any reactivity when treated with an excess of I^- ions. A rationalization of these results is provided in the Discussion section.

(21) Mastragostino, M.; Valcher, S.; Lazzari, P. *J. Electroanal. Chem. Interfacial Electrochem.* 1981, 126, 189.

(22) Bard, A. J.; Faulkner, L. R. *Electrochemical Methods*; Wiley: New York, 1980; p 701.

(d) Treatment of $\text{Cp}^*{}_{\text{2}}\text{Mo}_2\text{Cl}_4$ with HX ($\text{X} = \text{Br}, \text{I}$). As stated previously, we initially attempted the generation of $\text{Cp}^*{}_{\text{2}}\text{Mo}_2\text{X}_4$ ($\text{X} = \text{Br}, \text{I}$) by halide exchange from the corresponding chloride system. We found the reaction of $\text{Cp}^*{}_{\text{2}}\text{Mo}_2\text{Cl}_4$ with NaI in THF to proceed only slightly whereas the corresponding reaction with NaBr did not proceed at all. We then turned to the utilization of HX in CH_2Cl_2 . This is known as an efficient method for exchanging a lighter halide with a heavier one in transition metal complexes and proceeds in the desired direction because the HX bond is much stronger when X is a lighter halide. For instance, this method has been used to convert MCl_n to MX_m ($\text{M} = \text{Ti}, \text{V}, \text{Mo}; n = 4; \text{M} = \text{Nb}, \text{Ta}; n = 5; \text{X} = \text{Br}, \text{I}$),^{23a-c} Au_2Cl_6 to Au_2Br_6 and $\{\text{AuI}\}_{\infty}$,^{23d} and also $\text{Re}_2\text{Cl}_8^{2-}$ to $\text{Re}_2\text{I}_8^{2-}$.²⁴

The interaction of $\text{Cp}^*{}_{\text{2}}\text{Mo}_2\text{Cl}_4$ with HX results, as expected, in halide exchange. However, the reactions are accompanied by oxidation, presumably by H^+ with evolution of H_2 . The reaction with HBr gives a solution which shows the characteristic resonances of $[\text{Cp}^*{}_{\text{2}}\text{Mo}_2\text{Br}_4]^+$ and $[\text{Cp}^*\text{MoBr}_4]^-$ in the $^1\text{H-NMR}$. There is no evidence for the presence, in this solution, of $\text{Cp}^*{}_{\text{2}}\text{Mo}_2\text{Br}_6$, but this compound would presumably react with the excess HBr present to afford the mononuclear tetrabromo anion (see the reaction of $\text{Cp}^*{}_{\text{2}}\text{Mo}_2\text{Br}_6$ with Br^- salts described later). The NMR properties of this solution were consistently reproduced. However, crystallization of the crude product from CH_2Cl_2 /heptane sometimes produced a crystalline material that exhibited the same NMR properties of the crude material, whereas other times it afforded crystals of $\text{Cp}^*{}_{\text{2}}\text{Mo}_2\text{Br}_6$ in two different polymorphs which were both investigated crystallographically. The crystals of the other species, presumably $[\text{Cp}^*{}_{\text{2}}\text{Mo}_2\text{Br}_4]^+[\text{Cp}^*\text{MoBr}_4]^-$, were found to be unsuitable for an X-ray diffraction study. To explain the variability of these recrystallization results, we can only imagine the involvement of a variable quantity of excess HBr. If a sufficient amount of excess HBr is present, this may prevent the formation of the neutral Mo(IV) dimer, whereas if HBr is present in smaller amounts or is extensively removed from the residue under a dynamic vacuum, then the formation of some $\text{Cp}^*{}_{\text{2}}\text{Mo}_2\text{Br}_6$ through the equilibrium shown in Scheme 1 would occur.

The reaction of $\text{Cp}^*{}_{\text{2}}\text{Mo}_2\text{Cl}_4$ with HI in CH_2Cl_2 proceeded rapidly with a color change to emerald green, which is the characteristic color of the $[\text{Cp}^*{}_{\text{2}}\text{Mo}_2\text{I}_4]^+$ ion. The isolated material from this reaction, however, shows elemental analysis, $^1\text{H-NMR}$ and cyclic voltammetric properties approximately midway between those expected for the triiodide salts of the $[\text{Cp}^*{}_{\text{2}}\text{Mo}_2\text{I}_4]^+$ and $[\text{Cp}^*{}_{\text{2}}\text{Mo}_2\text{Cl}_4]^+$ ions. The presence of I_3^- as a counterion is clearly visible from the cyclic voltammogram. Bubbling of HI for a short (5 min) or long (1 h) period did not make a difference in the $^1\text{H-NMR}$ spectrum of the resulting solution. A single crystal grown from this solution confirmed the formulation of the compound as $[\text{Cp}^*{}_{\text{2}}\text{Mo}_2(\mu\text{-Cl})_x(\mu\text{-I})_{4-x}]^+\text{I}_3^-$ (vide infra), with $x = 2$ from refinement of the X-ray data, in accord with the analytical and spectroscopic observations.

(e) Reaction of Various Forms of Cp^*MoX_3 with X^- and Characterization of $[\text{Cp}^*\text{MoX}_4]^-$. Treatment of the mixture of compounds that is obtained from the thermal decarbonylation in CH_2Cl_2 (containing $\text{Cp}^*{}_{\text{2}}\text{Mo}_2\text{Br}_6$, $[\text{Cp}^*{}_{\text{2}}\text{Mo}_2\text{Br}_4]^+[\text{Cp}^*\text{MoBr}_4]^-$ and Cp^*MoBr_4 , see Scheme 1) with excess bromide ion slowly affords $[\text{Cp}^*\text{MoBr}_4]^-$ as the only $^1\text{H-NMR}$ active species. The $^1\text{H-NMR}$ monitoring of this reaction gives valuable information on the different chemical reactivity of the various solution species. The $^1\text{H-NMR}$ resonance of $\text{Cp}^*{}_{\text{2}}\text{Mo}_2\text{Br}_6$ disappears immediately

and the resonance of $[\text{Cp}^*\text{MoBr}_4]^-$ correspondingly increases in intensity, whereas the resonance of $[\text{Cp}^*{}_{\text{2}}\text{Mo}_2\text{Br}_4]^+$ decreases over a much longer time scale (several days at room temperature) and eventually disappears. These observations indicate that only $\text{Cp}^*{}_{\text{2}}\text{Mo}_2\text{Br}_6$ is able to react rapidly with donor ligands and the other solution species are consumed presumably only through the establishment of the slow equilibrium with $\text{Cp}^*{}_{\text{2}}\text{Mo}_2\text{Br}_6$. Consistent with this view, the reaction between $[\text{Cp}^*{}_{\text{2}}\text{Mo}_2\text{Br}_4]^-(\text{Br}^-)_x(\text{Br}_3^-)_{1-x}$ (x ca. 0.2) and excess Br^- also slowly affords $[\text{Cp}^*\text{MoBr}_4]^-$ as the only $^1\text{H-NMR}$ active species, and no observable accumulation of $\text{Cp}^*{}_{\text{2}}\text{Mo}_2\text{Br}_6$ is observed by $^1\text{H-NMR}$ monitoring.

On a preparative scale, compound $n\text{-Bu}_4\text{N}^+[\text{Cp}^*\text{MoBr}_4]^-$ has been obtained in excellent yields by adding the stoichiometric amount of Br^- to the material obtained from the thermal decarbonylation of $\text{Cp}^*\text{MoBr}_3(\text{CO})_2$ in refluxing dichloromethane. Therefore, although this material of approximate composition Cp^*MoBr_3 is in reality a complicated mixture of different species, indeed it represents a convenient source of the Cp^*MoBr_3 synthon. The analogous reaction between $\text{Cp}^*{}_{\text{2}}\text{Mo}_2\text{I}_6$ (purple Cp^*MoI_3) and salts of I^- gives an immediate change of color to dark green, accompanied by the replacement of the $^1\text{H-NMR}$ resonance of the starting material by that of the product $[\text{Cp}^*\text{MoI}_4]^-$ (Figure 1). This complex has been isolated as Bu_4N and Me_3PhN salts, the latter of which has been characterized crystallographically (vide infra). The $^1\text{H-NMR}$ resonance observed for the $[\text{Cp}^*\text{MoX}_4]^-$ ($\text{X} = \text{Br}, \text{I}$) anions around $\delta = -19.5$ and -21.7 , respectively (cf. $\delta = -13.5$ for the corresponding ion with $\text{X} = \text{Cl}$),⁹ shows that these 16-electron complex are paramagnetic, thus presumably having two unpaired electrons, as proven to be the case for the isostructural and isoelectronic $\text{Cp}^*\text{MoCl}_3(\text{PMe}_3)$ by magnetic susceptibility measurements.¹⁵

The Mo(IV) anion $[\text{Cp}^*\text{MoBr}_4]^-$ undergoes a reversible one-electron oxidation to give the neutral Mo(V) complex Cp^*MoBr_4 ($E_{1/2} = -0.14$ V vs $\text{Cp}_2\text{Fe}/\text{Cp}_2\text{Fe}^+$), which compares with the corresponding process at -0.16 V for $[\text{Cp}^*\text{MoCl}_4]^-$ (see Figure 2).⁹ The redox behavior of the $[\text{Cp}^*\text{MoI}_4]^-$ anion, however, is different. An *irreversible* oxidation wave at $E_{p,a} = -0.14$ V is observed, followed at more positive potentials by a reversible oxidation at ca. $E_{1/2} = +0.22$ V. These processes correspond to the oxidation of I^- to I_3^- and then to I_2 (see Figure 2). At yet higher potentials a reversible oxidation wave is observed ($E_{1/2} = +0.49$ V), corresponding to the $[\text{Cp}^*{}_{\text{2}}\text{Mo}_2\text{I}_4]^+/\text{[Cp}^*{}_{\text{2}}\text{Mo}_2\text{I}_4]^{2+}$ process. The same processes are also observed in the cyclic voltammogram of $\text{Cp}^*{}_{\text{2}}\text{Mo}_2\text{I}_6$. It appears, therefore, that the electrochemistry of these Mo(IV) systems are dominated by the I^- ion, presumably because of a rapid, although not necessarily extensive, dissociation equilibrium of the ion from Mo(IV). The CV experiments described above also illustrate that electrochemical oxidation, like chemical oxidation by I_2 , induces the transformation of the Mo(IV) material into the more reduced $[\text{Cp}^*{}_{\text{2}}\text{Mo}_2\text{I}_4]^+$ ion. These CV experiments therefore demonstrate the thermodynamic instability of the hypothetical neutral Mo(V) complex Cp^*MoI_4 , since the redox potential for the hypothetical $\text{Cp}^*\text{MoI}_4/\text{[Cp}^*\text{MoI}_4]^-$ couple would be more positive than the potential necessary to oxidize I^- to I_3^- (see Figure 2).

Contrary to the observed reaction of Br^- with all forms of " Cp^*MoBr_3 " (even the salt $[\text{Cp}^*{}_{\text{2}}\text{Mo}_2\text{Br}_4]^+(\text{Br}^-)_x(\text{Br}_3^-)_{1-x}$ is slowly converted to $[\text{Cp}^*\text{MoBr}_4]^-$ through the equilibration with the more reactive $\text{Cp}^*{}_{\text{2}}\text{Mo}_2\text{Br}_6$ compound), no reaction takes place between I^- and $[\text{Cp}^*{}_{\text{2}}\text{Mo}_2\text{I}_4]^+(\text{I}^-)_{0.5}(\text{I}_3^-)_{0.5}$. This observation indicates that the transformation of purple Cp^*MoI_3 to green Cp^*MoI_3 is irreversible because, as shown above, purple Cp^*MoI_3 reacts readily and quantitatively with I^- .

(f) Reaction of Various Forms of Cp^*MoX_3 with Other 2e Donors. The reaction of different forms of Cp^*MoX_3 with CO has been studied only qualitatively with IR monitoring. The results obtained reinforce the idea that only the neutral $\text{Cp}^*{}_{\text{2}}$

(23) (a) Biagini, P.; Calderazzo, F.; Pampaloni, G.; Zanazzi, P. F. *Gazz. Chim. Ital.* 1987, 117, 27. (b) Calderazzo, F.; Pallavicini, P.; Pampaloni, G.; Zanazzi, P. F. *J. Chem. Soc., Dalton Trans.* 1990, 2743. (c) Calderazzo, F.; Maichle-Mössmer, C.; Pampaloni, G.; Strähle, J. *J. Chem. Soc., Dalton Trans.* 1993, 655. (d) Belli Dell'Amico, D.; Calderazzo, F.; Morvillo, A.; Pelizzi, G.; Robino, P. *J. Chem. Soc., Dalton Trans.* 1991, 3009.

(24) Preetz, W.; Rudzik, L. *Angew. Chem., Int. Ed. Engl.* 1978, 18, 150.

Mo_2X_6 species is the reactive form for ligand addition reactions. Due to the small amounts of material obtained, the reaction of pure $\text{Cp}^*\text{}_2\text{Mo}_2\text{Br}_6$ with CO has not been investigated. On the other hand, CO reacts with a mixture of $\text{Cp}^*\text{}_2\text{Mo}_2\text{Br}_6$, $[\text{Cp}^*\text{}_2\text{Mo}_2\text{Br}_4]^+[\text{Cp}^*\text{MoBr}_4]^-$, and Cp^*MoBr_4 compounds in CH_2Cl_2 to immediately generate $\text{Cp}^*\text{MoBr}_3(\text{CO})_2$, as shown by solution IR spectroscopy, whereas no immediate reaction occurs when exposing a CH_2Cl_2 solution of $[\text{Cp}^*\text{}_2\text{Mo}_2\text{Br}_4]^+(\text{Br}^-)_x(\text{Br}_2^-)_{1-x}$ to an atmosphere of CO. In the latter reaction, the IR bands of the dicarbonyl product could be observed after an overnight stirring at room temperature. As for the reaction with Br^- discussed in the previous section, this can be ascribed to the slow equilibration reaction of the salt with the neutral $\text{Cp}^*\text{}_2\text{Mo}_2\text{Br}_6$ compound.

For the iodide system, $\text{Cp}^*\text{}_2\text{Mo}_2\text{I}_6$ reacts with CO in CH_2Cl_2 with rapid quenching of the purple color, and the resulting pale brown solution shows the CO stretching vibrations of the compound $\text{Cp}^*\text{MoI}_3(\text{CO})_2$. On the other hand, neither $[\text{Cp}^*\text{}_2\text{Mo}_2\text{I}_4]^-(\text{I}^-)_0(\text{I}_3^-)_{0.5}$ nor $[\text{Cp}^*\text{}_2\text{Mo}_2\text{I}_4]^+(\text{I}_3^-)$ exhibits any reactivity with CO in CH_2Cl_2 , even upon prolonged exposure. As for the lack of reaction with I^- , this observation is consistent with a much greater thermodynamic stability of the green vs the purple form of Cp^*MoI_3 .

The reaction with PMe_3 has also been investigated. The mixture of compounds obtained by decarbonylating $\text{Cp}^*\text{MoBr}_3(\text{CO})_2$ in CH_2Cl_2 reacts with the stoichiometric amount of PMe_3 to afford $\text{Cp}^*\text{MoBr}_3(\text{PMe}_3)$. The product has been isolated only in small yields, but the $^1\text{H-NMR}$ monitoring shows the complete consumption of all observable components of the starting mixture of Cp^*Mo compounds. The analogous $\text{Cp}^*\text{MoCl}_3(\text{PMe}_3)$ compound was similarly obtained by addition of PMe_3 to $\text{Cp}^*\text{}_2\text{Mo}_2\text{Cl}_6$.⁹ The $^1\text{H-NMR}$ properties of these 16-electron $\text{Cp}^*\text{MoX}_3(\text{PMe}_3)$ materials are consistent with the presence of two unpaired electrons and have been described in detail in a previous report.¹⁵ The reaction of Cp^*MoI_3 compounds with PMe_3 takes a different course. As mentioned earlier, Parkin was first to discover¹⁶ that clean reduction to $\text{Cp}^*\text{}_2\text{Mo}_2\text{I}_4$ occurs upon treatment of green Cp^*MoI_3 with PMe_3 . Addition of PMe_3 to $\text{Cp}^*\text{}_2\text{Mo}_2\text{I}_6$ also affords the Mo(III) reduction product, but several other paramagnetic compounds, one of which may be the 16-electron $\text{Cp}^*\text{MoI}_3(\text{PMe}_3)$ compound, are also formed as indicated by $^1\text{H-NMR}$ spectrometry (see Experimental Section for details). This reaction was not investigated further.

(g) Conproportionation of $\text{Cp}^*\text{}_2\text{Mo}_2\text{Br}_4$ and Cp^*MoBr_4 . The reaction between $\text{Cp}^*\text{}_2\text{Mo}_2\text{Cl}_4$ and Cp^*MoCl_4 has been described before as one of the methods for the formation of $\text{Cp}^*\text{}_2\text{Mo}_2\text{Cl}_6$ and its NMR monitoring has given valuable insights into the mechanism of this transformation.⁹ The electrochemical properties of the $\text{Cp}^*\text{}_2\text{Mo}_2\text{X}_4$ and Cp^*MoX_4 complexes (Figure 2) allow one to predict that the interaction between these complexes in a 1:1 ratio will result in electron transfer with formation of the $[\text{Cp}^*\text{}_2\text{Mo}_2\text{X}_4]^+[\text{Cp}^*\text{MoX}_4]^-$ salt. Indeed, mixing equimolar amounts of $\text{Cp}^*\text{}_2\text{Mo}_2\text{Br}_4$ and Cp^*MoBr_4 in CD_2Cl_2 leads to the immediate development of the $^1\text{H-NMR}$ resonances of the $[\text{Cp}^*\text{}_2\text{Mo}_2\text{Br}_4]^+$ and $[\text{Cp}^*\text{MoBr}_4]^-$ species with complete disappearance of the resonance due to the Mo(III) starting material (the Mo(V) starting material is NMR silent). Surprisingly, we found that the resulting solution is stable and gives rise to no new $^1\text{H-NMR}$ resonance even after 1 week at room temperature. Only upon addition of a second equivalent of Cp^*MoBr_4 is the equilibrium mixture indicated in Scheme 1 slowly obtained, ($[\text{Cp}^*\text{}_2\text{Mo}_2\text{Br}_4]^+[\text{Cp}^*\text{MoBr}_4]^-/\text{Cp}^*\text{}_2\text{Mo}_2\text{Br}_6$ ratio = 4.8 ± 0.2). This behavior contrasts markedly with that of the $[\text{Cp}^*\text{}_2\text{Mo}_2\text{Cl}_4]^+[\text{Cp}^*\text{MoCl}_4]^-$ solution obtained by 1:1 interaction of $\text{Cp}^*\text{}_2\text{Mo}_2\text{Cl}_4$ and Cp^*MoCl_4 , which rapidly affords a mixture of $\text{Cp}^*\text{}_2\text{Mo}_2\text{Cl}_6$ and $\text{Cp}^*\text{}_2\text{Mo}_2\text{Cl}_5$ via a chloride transfer process, and the addition of a second equivalent of Cp^*MoCl_4 ultimately leads to $\text{Cp}^*\text{}_2\text{Mo}_2\text{Cl}_6$ as the only reaction product.⁹

(h) $^1\text{H-NMR}$ Properties of $\text{Cp}^*\text{}_2\text{Mo}_2\text{X}_6$. Is There a Second Isomeric Form in Solution? The $^1\text{H-NMR}$ resonances observed at ca. δ -6.0 and -5.1 (CD_2Cl_2) for isolated $\text{Cp}^*\text{}_2\text{Mo}_2\text{X}_6$ ($\text{X} = \text{Br}$ and I, respectively) are in accord with the solid state structure found for the bromide compound (structure I, *vide infra*). The corresponding chloride compound, which also adopts structure I, shows its $^1\text{H-NMR}$ resonance at ca. δ -4.2 in the same solvent. As discussed in the previous paper reporting our studies on $\text{Cp}^*\text{}_2\text{Mo}_2\text{Cl}_6$,⁹ a solution mononuclear 14-electron Cp^*MoX_3 species is not possible and the observation of one resonance is not consistent with trinuclear structures. The metal coordination geometry and electronic configuration in the $\text{Cp}^*\text{}_2\text{Mo}_2\text{X}_6$ molecules (16-electron four-legged piano stool) are identical to those in the corresponding $[\text{Cp}^*\text{MoX}_4]^-$ anions (see structural section later for details), but the Cp^* proton resonances in the dinuclear neutral complexes have a much reduced paramagnetic shift in the $^1\text{H-NMR}$ with respect to those of the mononuclear anions (see Figure 1). This is consistent with the magnetic properties of the dinuclear and mononuclear complexes, since the NMR paramagnetic shift is known to be proportional to the magnetic susceptibility, and the room temperature magnetic moment of $\text{Cp}^*\text{}_2\text{Mo}_2\text{I}_6$ ($1.61 \mu_B$ per Mo atom) is close to that reported for $\text{Cp}^*\text{}_2\text{Mo}_2\text{Cl}_6$ ($1.40 \mu_B$ per Mo atom)⁹ but reduced with respect to the moment expected for magnetically noninteracting metal atoms (spin-only value = $2.83 \mu_B$). This phenomenon is consistent with antiferromagnetic coupling, as verified for the chloride compound by variable temperature magnetic susceptibility and $^1\text{H-NMR}$ studies.⁹ Spin-orbit coupling effects appear to be small for the four-legged piano stool geometry, since the moment measured for $\text{Cp}^*\text{MoX}_3(\text{PMe}_3)$ is $2.63 \mu_B$ (temperature independent) for $\text{X} = \text{Cl}^9$ and $2.74 \mu_B$ for $\text{X} = \text{Br}$. The slight increase of moment on going from the chloro to the iodo complex is most likely due to the expected greater Mo-Mo separation in the iodo material due to the larger size of the bridging halide ligands. Unfortunately, we could not obtain a sufficient amount of pure $\text{Cp}^*\text{}_2\text{Mo}_2\text{Br}_6$ material for a magnetic susceptibility study.

A minor, sharp resonance at δ 2.09 in CDCl_3 was always observed in those $^1\text{H-NMR}$ spectra where the resonance of $\text{Cp}^*\text{}_2\text{Mo}_2\text{Br}_6$ was also present at δ -5.7 (typically, the integrated intensity of this diamagnetic resonance is <10% with respect to that at δ -5.7). The same phenomenon is exhibited by the chloro analogue,⁹ for which a diamagnetic resonance at δ 1.98 accompanies the paramagnetically shifted resonance of $\text{Cp}^*\text{}_2\text{Mo}_2\text{Cl}_6$ (structure I) at δ -3.87. We initially suspected that this resonance could be due to a diamagnetic isomeric form of the dimer having structure II. Structures I and II both feature a four-legged piano stool coordination geometry around the metal atoms and the two stools share two legs to give rise, respectively, to an *anti* and a *syn* configuration. Structure II has a much better disposition of the metal orbitals to form metal-metal bonds and therefore could give rise to a diamagnetic compound. This idea originates from the observation that the *paramagnetic* d^1-d^1 compound $(\text{C}_5\text{Me}_4\text{Et})_2\text{Ta}_2\text{Br}_6$ adopts structure I with no Ta-Ta bond,²⁵ whereas the *diamagnetic* d^3-d^3 compound $(\text{C}_5\text{Me}_4\text{Et})_2\text{Re}_2\text{Cl}_6$ adopts structure II with a Re-Re bond.²⁶ Therefore, an equilibrium between the two structures could be adopted for the d^2-d^2 Mo compounds. In apparent agreement with this idea is also the observation, in general, of greater proportions of this diamagnetic resonance for the chloro system with respect to the bromo system and the absence of such a diamagnetic resonance for the iodo system (a smaller bridging halide would favor metal-metal bond formation in structure II). However, some results of our previous studies on the chloro system seem in contrast with this idea.⁹ A partial hydrolysis process or a reaction with the chlorinated NMR solvent are possibilities to be taken into account, but so far the exact nature of the species that gives rise to this

(25) Ting, C.; Messerle, L. *Inorg. Chem.* 1989, 28, 171.

(26) Herrmann, W. A.; Fischer, R. A.; Felixberger, J. K.; Paciello, R. A.; Kiprof, P.; Herdtweck, E. Z. *Naturforsch.* 1988, 43B, 1391.

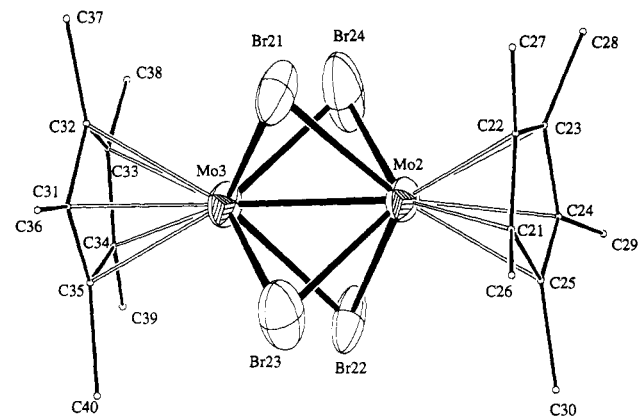
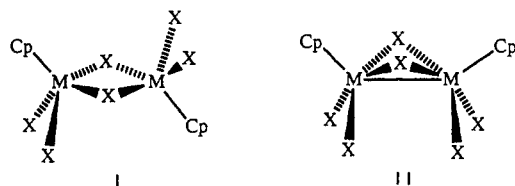


Figure 3. ORTEP view of the $[Cp^*_2Mo_2Br_4]^+$ ion in compound $\{[Cp^*_2Mo_2Br_4]^+[Cp^*MoBr_4]^-_2\}_2 \cdot Cp^*MoBr_4$. Ellipsoids are drawn at the 40% probability level. Hydrogen atoms are omitted and carbon atoms are drawn with arbitrary radii for clarity. The geometry of the molecule is identical to that observed for the corresponding neutral species, $Cp^*_2Mo_2Br_4$, a view of which is available in our preliminary communication.¹²

resonance remains unknown. Whatever the source of this diamagnetic resonance, this has not affected the reactions of the $Cp^*_2Mo_2X_6$ compounds, including the compound with $X = Cl$, that we have investigated so far.



Molecular Structures

The structures of the following compounds have been determined in this study: $Cp^*_2Mo_2Br_4$, $Cp^*_2Mo_2Br_6$ (three forms, two polymorphs without interstitial solvent and one with an interstitial benzene molecule per Mo_2 unit), $\{[Cp^*_2Mo_2Br_4] \cdot [Cp^*MoBr_4]\}_2 \cdot Cp^*MoBr_4$ (with two heptane molecules of crystallization per formula unit), $[Cp^*_2Mo_2Br_4]I_3$, $[Me_3PhN][Cp^*MoI_4]$ and a mixed-halide compound $[Cp^*_2Mo_2Cl_xI_{4-x}]I_3$. The structures of $Cp^*_2Mo_2Br_4$,¹³ $\{[Cp^*_2Mo_2Br_4] \cdot [Cp^*MoBr_4]\}_2 \cdot Cp^*MoBr_4$,¹³ and $[Cp^*_2Mo_2I_4]I_3$,¹² have been previously communicated.

The structure of $Cp^*_2Mo_2Br_4$ consists of two independent molecules in space group $P2_1/n$, one in a general position and a second one sitting on a crystallographic inversion center (positional parameters are given in Table 5 and selected bonding parameters in Table 6). The two polymorphs of $Cp^*_2Mo_2Br_6$ are respectively in space groups $C2/c$ and $P2_1/n$, both with the molecule residing on a crystallographic inversion center (positional parameters in Table 2, selected bond distances and angles in Table 3). The benzene solvate $Cp^*_2Mo_2Br_6 \cdot C_6H_6$ also exhibits the Mo dimer on an inversion center in $P2_1/n$ (data in Tables 3 and 4). The $\{[Cp^*_2Mo_2Br_4]^+[Cp^*MoBr_4]^-_2\}_2 \cdot Cp^*MoBr_4$ compound crystallizes in $P2_1/m$ with the cation in a general position and the three mononuclear fragments all sitting on crystallographic mirror planes in three different locations (data in Tables 7 and 8). The redox potentials of the $[Cp^*_2Mo_2Br_4]^{n/n+1}$ ($n = 0, +1$) and $[Cp^*MoBr_4]^{0/-}$ processes, summarized in Figure 2, unequivocally establish the distribution of charges given for this materials and rules out the alternative formulation as a 1:1 mixture of dinuclear mono- and dications with three mononuclear Mo(IV) anions. The structure is of rather low quality given the poorly diffracting crystal and the presence of a disordered heptane molecule in the lattice. Nevertheless, the structural determination of this compound has been key to this study, in particular to prove the presence of both the $[Cp^*_2Mo_2Br_4]^+[Cp^*MoBr_4]^-$ and the neutral Cp^*MoBr_4 in equilibrium with the neutral Mo(IV) dimer Cp^*_2-

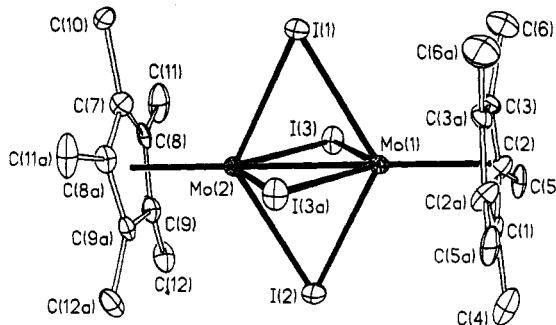


Figure 4. ORTEP view of the cation in the structure of $[Cp^*_2Mo_2I_4]^+I_3^-$. Ellipsoids are drawn at the 35% probability level. Hydrogen atoms are omitted for clarity. The same geometry is observed for the disordered cation in the structure of $[Cp^*_2Mo_2Cl_xI_{4-x}]^+I_3^-$.

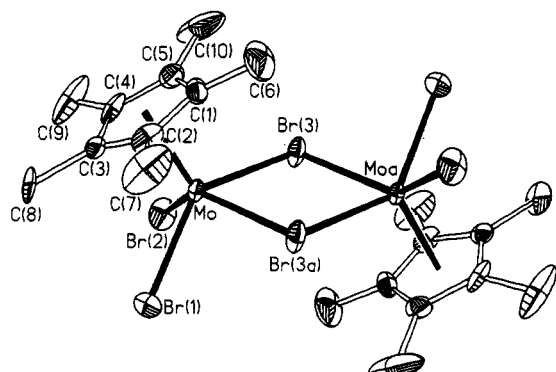


Figure 5. ORTEP view of the $Cp^*_2Mo_2Br_6$ molecule. Ellipsoids are drawn at the 35% probability level. Hydrogen atoms are omitted for clarity. The unsolvated $C2/c$ polymorph (I) is shown here. The three $Cp^*_2Mo_2Br_6$ structures are geometrically identical. The numbering scheme is identical for the other two structures.

Mo_2Br_6 in solution (see Scheme 1). The molecules are arranged in such a way as to form separate stacks of cations, anions, and neutral molecules along the b axis (see a drawing of the unit cell contents in Figure 4 of ref 13). The cations, anions, and neutral species are all well separated from each other. The $[Cp^*_2Mo_2Cl_xI_{4-x}]I_3$ ($x = 0, 2$) compounds both crystallize in the orthorhombic system, the compound with $x = 0$ in space group $Cmc2_1$ with both ions being located on a mirror plane (Tables 9 and 10), and the compound with $x = 2$ in space group $Pn2_1a$ with the entire molecule in the asymmetric unit (Tables 10 and 11). The I_3^- anion is, as expected, practically linear and fairly symmetric around the central iodine atom in both structures. Finally, $[Me_3PhN][Cp^*MoI_4]$ crystallizes in monoclinic $P2_1/c$ with two chemically equivalent independent molecules in the asymmetric unit (positional parameters in Table 12 and bonding parameters in Table 13). All in all, these structures show the geometry and bonding parameters of the following molecules and ions in order of increasing oxidation states: $Mo(III)$ species, $Cp^*_2Mo_2Br_4$; mixed-valence $Mo_2(III,IV)$ species, $[Cp^*_2Mo_2X_4]^+ [X = Br$ (Figure 3), I (Figure 4) or $X_4 = Cl_2I_2$]; $Mo(IV)$ species, $Cp^*_2Mo_2Br_6$ (Figure 5) and $[Cp^*MoX_4]^- [X = Br, I$ (Figure 6)]; $Mo(V)$ species, Cp^*MoBr_4 .

The coordination geometry around the central metal atom is of the four-legged piano stool type for all the structures described here. The metal is able to accommodate different oxidation states within the same structural motif by sharing a different number of halide atoms with another metal (four for the Mo^{IV}_2 and Mo^{III} Mo^{IV} compounds; two for the Mo^{IV}_2 compounds and zero for the mononuclear $Mo(IV)$ and $Mo(V)$ compounds). The quadruply-bridged dinuclear structure shown for $Cp^*_2Mo_2Br_4$ and $[Cp^*_2Mo_2X_4]^+ (X = Br, I or X_4 = Cl_2I_2)$ (Figures 3 and 4) is analogous to those described for other group 5 and 6 cyclopentadienylhafometal complexes, i.e. $(\eta^5-C_5H_4-i-Pr)_2Mo_2Cl_4$,^{2a} $(\eta^5-C_5Me_4-Et)_2Mo_2Cl_4$,¹⁹ $Cp^*_2W_2Cl_4$,²⁷ $\#Cp^*Mo_2Br_4$ ($\#Cp = \eta^5-1-(2,5-$

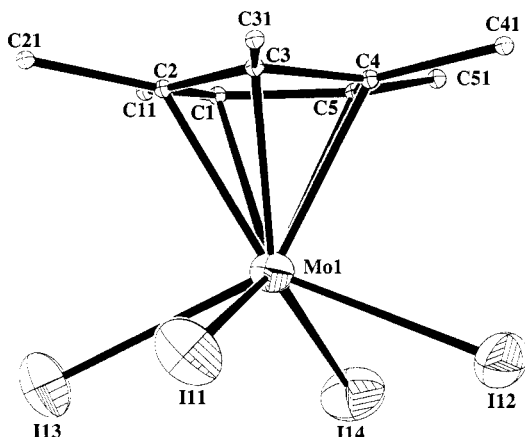


Figure 6. ORTEP view of one of the two independent $[\text{Cp}^*\text{MoI}_4]^-$ anions. Ellipsoids of the Mo and I atoms are drawn at the 40% probability level, whereas carbon atoms are drawn as spheres with a common arbitrary radius. Hydrogen atoms are omitted for clarity. The geometry of the complex is identical to that observed for the other $[\text{Cp}^*\text{MoI}_4]^-$ ion in this structure, and also for the two crystallographically independent $[\text{Cp}^*\text{Mo}_2\text{Br}_4]^-$ ions and for the neutral Cp^*MoBr_4 complex in the structure of compound $\{[\text{Cp}^*\text{Mo}_2\text{Br}_4]^+[\text{Cp}^*\text{MoBr}_4]\}_2\cdot\text{Cp}^*\text{MoBr}_4$. A view of the neutral Cp^*MoBr_4 complex is available in our preliminary communication.¹²

dimethoxyphenyl)-2,3,4,5-tetraphenylcyclopentadienyl),²⁰ and $\text{Cp}^*\text{Ta}_2\text{Br}_4$.²⁸ Also related to these complexes are other quadruply bridged structures, e.g. with four bridging thiolate ligands.²⁹ The structure of $[\text{Cp}^*\text{Mo}_2\text{I}_4]^+$, reported in full here,¹³ is the first structure with four bridging iodide ligands from any two metals. For the mixed-halide $[\text{Cp}^*\text{Mo}_2\text{Cl}_x\text{I}_{4-x}]^+$, each of the four bridging positions has Cl/I disorder. Free refinement of the Cl and I occupancies (with the constraint of an overall four-atom stoichiometry) gave the Cl/I composition at each individual bridging position and a value of $x = 2$, which corresponds to that independently obtained from the fitting of the C, H analytical values. The geometry of $\text{Cp}^*\text{Mo}_2\text{Br}_6$ (Figure 5) is identical to that of the corresponding $\text{Cp}^*\text{Mo}_2\text{Cl}_6$ compound,⁹ with the (nonbonded) metal–metal separation increasing from 3.888(1) to 4.098[26] Å (average of the three independent structures) on going from chloro to bromo complex, this increase being attributed to the larger size of the bridging bromine atoms. The bonding parameters in the three crystalline forms of this complex are very similar (see Table 3). Finally, no structure of a tetrahalocyclopentadienylmolybdate(IV) anion, or of a tetrahalocyclopentadienylmolybdenum(V), had been previously reported. Similar mononuclear structures for other metals are those of $(\text{C}_5\text{H}_4\text{-}i\text{-Pr})\text{WCl}_4$ ^{2b} and Cp^*TaBr_4 .³⁰ To the best of our knowledge, $[\text{Cp}^*\text{MoI}_4]^-$ is the first cyclopentadienyltetraiodo complex to be reported and structurally characterized.

The distortions of the four-legged piano stool geometry can be quantified from the values of the trans CNT–Mo–X angles. These are smaller for the mononuclear species (Cp^*MoBr_4 , 111(2)°; $[\text{Cp}^*\text{MoBr}_4]^-$, 112(3)°; $[\text{Cp}^*\text{MoI}_4]^-$, 113(1)°) and for $\text{Cp}^*\text{Mo}_2\text{Br}_6$ (112.7(9)°), and larger for the quadruply-bridged dimers ($\text{Cp}^*\text{Mo}_2\text{Br}_4$, 120.4(6); $[\text{Cp}^*\text{Mo}_2\text{Br}_4]^+$, 120(1); $[\text{Cp}^*\text{Mo}_2\text{I}_4]^+$, 119.2(6)°; $[\text{Cp}^*\text{Mo}_2\text{Cl}_x\text{I}_{4-x}]^+$, 119(2)°). The former are more typical of four-legged piano stool structures with halide ligands,³¹ whereas the latter ones are somewhat expanded, undoubtedly

Table 14. Mo–Mo Distances in Known Dinuclear Complexes of Structure [(ring)Mo(μ -X)Mo(ring)] n^+ ($n = 0, 1$; X = halogen)

complex	d ⁿ –d ⁿ configuration	dist, Å	ref
$(\text{C}_5\text{H}_4\text{-}i\text{-Pr})_2\text{Mo}_2\text{Cl}_4$	d ³ –d ³	2.607(1)	2a
$(\text{C}_5\text{Me}_4\text{Et})_2\text{Mo}_2\text{Cl}_4$	d ³ –d ³	2.600(2), 2.596(2)	19
$\text{Cp}^*\text{Mo}_2\text{Br}_4$	d ³ –d ³	2.691(4)	20
$\text{Cp}^*\text{Mo}_2\text{Br}_4$	d ³ –d ³	2.654(2), 2.641(4)	this work
$[\text{Cp}^*\text{Mo}_2\text{Br}_4]^+$	d ² –d ³	2.643(5)	this work
$\text{Cp}^*\text{Mo}_2\text{I}_4$	d ³ –d ³	2.708(3)	16b
$[\text{Cp}^*\text{Mo}_2\text{I}_4]^+$	d ² –d ³	2.718(3)	this work
$[\text{Cp}^*\text{Mo}_2\text{Cl}_2\text{I}_2]^+$	d ² –d ²	2.658(2)	this work

due to the geometric requirements imposed by the formation of the metal–metal bond in the quadruply-bridged species. The CNT–Mo–X angle, in the absence of complicating Mo–Mo bonding factors, is diagnostic of the spin state for 16-electron systems when the ligand involved is a π donor such as Br and I.³¹ In low spin complexes such as $(\eta^6\text{-C}_7\text{H}_7\text{SiMe}_3)_2\text{ZrI}_2(\text{PMMe}_3)_2$ the CNT–Zr–I angles are large (>125°)³² because these atoms tend to maximize their π overlap with the empty metal d_{z²} orbital, whereas in high-spin complexes (containing one unpaired electron in each of the metal d_{xy} and d_{z²} orbitals) the two possible π interactions are competing with each other and lower angles result. Therefore, the CNT–Mo–X angles observed for the $[\text{Cp}^*\text{MoX}_4]^-$ (X = Br, I) and $\text{Cp}^*\text{Mo}_2\text{Br}_6$ structures are fully consistent with the high-spin configuration which is indicated by the ¹H-NMR spectrum.

The most interesting bonding parameter to be examined is the metal–metal distance in the quadruply-bridged species. A collection of all known Mo–Mo distances in quadruply-bridged complexes is shown in Table 14. This table shows that the Mo–Mo distance is most sensitive to the nature of the bridging groups, with the shorter distances for the tetrachloro-bridged complexes and the longer ones for the tetraiodo-bridged ones. The tetrabromo- and mixed-chloroiodo-bridged compounds show distances intermediate between the two extremes. The other interesting observation is the little or no dependence of the Mo–Mo distance on the electronic configuration (d³–d³ vs d²–d³). This is in agreement with recent theoretical prediction by Green *et al.*, according to which the d³–d³ configuration gives rise of a metal–metal single bond of configuration $\sigma^2\delta^*2\delta^2$. Upon one-electron oxidation, the electron is removed from an orbital which is substantially Mo–Mo nonbonding and therefore no dramatic effect on the metal–metal distance is expected.³³

The Mo–Br distances in the various structures reported in this contribution show a general shortening as the oxidation state on the metal is increased from III to V and other expected trends can also be observed (e.g. bonds to bridging Br ligands are longer than those to terminal ones in $\text{Cp}^*\text{Mo}_2\text{Br}_6$; bonds in anionic $[\text{Cp}^*\text{MoBr}_4]^-$ are longer than those to terminal Br ligands in the neutral dimer). The individual averages are as follows (b = bridging; t = terminal): Mo(III)–Br_b, 2.614(9) Å; Mo^{IV}–Br_b, 2.644(27) Å, Mo(IV)–Br_b, 2.615(9) Å; Mo(IV)–Br_t (neutral), 2.530(7) Å; Mo(IV)–Br_t (anionic), 2.62(4) Å; Mo(V)–Br_t, 2.48(3) Å. Following the same trend, the Mo–I distances are longer in the $[\text{Cp}^*\text{MoI}_4]^-$ anion (average 2.804(7) Å) with respect to the $[\text{Cp}^*\text{Mo}_2\text{I}_4]^+$ cation (average 2.787(9) Å). Due to the I/Cl disorder in the $[\text{Cp}^*\text{Mo}_2\text{Cl}_x\text{I}_{4-x}]^+$ ion, the Mo–X (X = mixture of Cl and I) distances obtained for this structure cannot be attributed any chemical meaning.

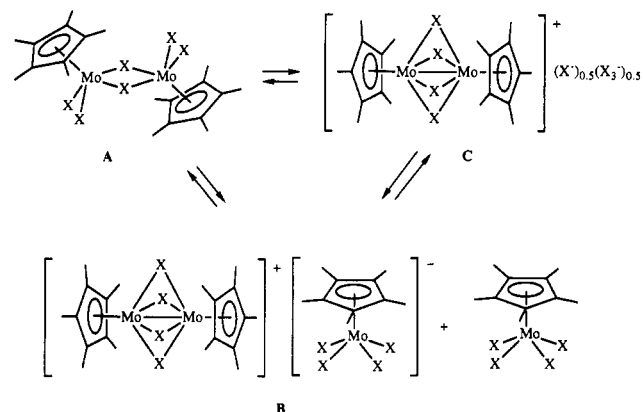
Given the similarity of Mo–Mo and Mo–Br distances between the two $[\text{Cp}^*\text{Mo}_2\text{Br}_4]^{n+}$ ($n = 0, 1$) species, it is no surprise that the oxidation of $\text{Cp}^*\text{Mo}_2\text{Br}_4$ is electrochemically reversible. In fact, the self-exchange reaction between the two species is rapid

- (27) Harlan, C. J.; Jones, R. A.; Koschmieder, S. U.; Nunn, C. M.; *Polyhedron* 1990, 9, 669.
 (28) Ting, C.; Baenziger, N. C.; Messerle, L. *J. Chem. Soc.* 1988, 1133.
 (29) (a) Connolly, N. G.; Dahl, L. F. *J. Am. Chem. Soc.* 1970, 92, 7470. (b) Rakowski DuBois, M.; Haltiwanger, R. C.; Miller, D. J.; Glatzmaier, G. *J. Am. Chem. Soc.* 1979, 101, 5245. (c) McKenna, M.; Wright, L. L.; Miller, D. J.; Tanner, L.; Haltiwanger, R. C.; Rakowski DuBois, M. *J. Am. Chem. Soc.* 1983, 105, 5329.
 (30) Messerle, L. Personal communication.
 (31) Poli, R. *Organometallics* 1990, 9, 1892.

(32) Green, M. L. H.; Mountford, P.; Walker, N. M. *J. Chem. Soc., Chem. Commun.* 1989, 908.

(33) Green, J. C.; Green, M. L. H.; Mountford, P.; Parkington, M. J. *J. Chem. Soc., Dalton Trans.* 1990, 3407.

Scheme 3



on the ^1H -NMR time scale (see Discussion). The Mo–Br bond length is the only parameter that allows us to identify the charge on the three mononuclear fragments in the $\{[\text{Cp}^*\text{Mo}_2\text{Br}_4]^+[\text{Cp}^*\text{MoBr}_4]^-)_2\cdot\text{Cp}^*\text{MoBr}_4$ structure; thus, the neutral Mo(V) complex corresponds to the fragment containing Mo(1), while the two fragments containing Mo(4) and Mo(5) correspond to the two anions. The oxidation of $[\text{Cp}^*\text{MoBr}_4]^-$ is also electrochemically reversible within the range of scan speeds investigated (50–500 mV/s) in spite of the large difference of Mo–Br distance between the two species, which is expected to introduce substantial reorganization during the redox process. However, the observation of the unshifted and unbroadened resonance of $[\text{Cp}^*\text{MoBr}_4]^-$ in the ^1H -NMR when Cp^*MoBr_4 is present (for instance, in the reaction between $\text{Cp}^*\text{Mo}_2\text{Br}_4$ and Cp^*MoBr_4 in a 1:2 ratio) indicates that the $[\text{Cp}^*\text{MoBr}_4]^-/\text{Cp}^*\text{MoBr}_4$ self-exchange is slow on the NMR time scale. This contrasts markedly with the situation for the chloro system, where the contemporary presence in solution of Cp^*MoCl_4 and $[\text{Cp}^*\text{MoCl}_4]^-$ causes the ^1H -NMR resonance of the anion to disappear completely.⁹

Discussion

It is useful to compare the chemistry reported here with that of the corresponding chloride system.⁹ A dinuclear trichloride compound, $\text{Cp}^*\text{Mo}_2\text{Cl}_6$, was obtained by either thermal decarbonylation of $\text{Cp}^*\text{MoCl}_3(\text{CO})_2$, reduction of Cp^*MoCl_4 with sodium amalgam or oxidation of the dimeric complex $\text{Cp}^*\text{Mo}_2\text{Cl}_4$ by PhICl_2 , and its formation was also observed by ^1H -NMR from the reaction between Cp^*MoCl_4 and $\text{Cp}^*\text{Mo}_2\text{Cl}_4$ in a 2:1 ratio. For the bromide and iodide systems, however, the analogous $\text{Cp}^*\text{Mo}_2\text{X}_6$ ($\text{X} = \text{Br}, \text{I}$) complexes can only be obtained under particular conditions and can be transformed, reversibly or irreversibly depending on the experimental conditions and on the nature of X , to other mixtures of compounds with the same overall “ Cp^*MoX_3 ” stoichiometry. These are illustrated in Scheme 3. We shall first discuss some structural/electrochemical correlations that will help rationalize the richness of structural motifs and the stability or instability of the different compounds encountered in this chemistry, and then turn to trends in reactivity and to mechanistic considerations.

(a) Structural Chemistry and Electrochemistry. One of our original interests was to ascertain whether a $d^2\text{Cp}^*\text{MoX}_3$ system would adopt a dinuclear, halide-bridged structure with a relative *anti* or *syn* arrangement of the two cyclopentadienyl rings (I or II). The four-legged piano stool structure has as metal-based frontier orbitals the d_{xy} and d_{z^2} orbitals³⁴ and our previous studies on four-legged piano stool Mo(IV) systems^{9,15,35} indicate that these inevitably adopt a high spin configuration. In other words, one metal electron is located in the d_{xy} orbital and the second one occupies the d_{z^2} orbital. Metal–metal overlap is expected to be

much better in structure II than in structure I. While the structures of the $d^1\text{--}d^1$ Ta(IV) compound $(\text{C}_5\text{Me}_4\text{Et})_2\text{Ta}_2\text{Br}_6$ is of type I with no metal–metal bond²⁵ and the $d^3\text{--}d^3$ Re(IV) dimer $(\text{C}_5\text{Me}_4\text{Et})_2\text{Re}_2\text{Cl}_6$ adopts structure II with a metal–metal-bonding interaction,²⁶ the structure of analogous $d^2\text{--}d^2$ systems were not known until we recently reported the structure of $\text{Cp}^*\text{Mo}_2\text{Cl}_6$,⁹ which is of type I and does not exhibit a metal–metal-bonding interaction. Solid state and solution studies demonstrate that the structure of the corresponding $\text{Cp}^*\text{Mo}_2\text{X}_6$ ($\text{X} = \text{Br}, \text{I}$) molecules is identical to that of the chloro system.

As we have already observed in Results, all the structures reported here show the ubiquitous four-legged piano stool geometry in all the oxidation states from III to V. When the oxidation state is increased, a greater number of X^- donors per metal (two for $[\text{Cp}^*\text{Mo}_2\text{X}_4]^{n+}$, three for $\text{Cp}^*\text{Mo}_2\text{X}_6$, and four for $[\text{Cp}^*\text{MoX}_4]^{n-}$), buffer the increase of positive charge on the metal center and the related increase of oxidizing power. As a result, the $E_{1/2}$ potential for the $[\text{Cp}^*\text{MoBr}_4]^-/\text{Cp}^*\text{MoBr}_4$ couple falls within the region of stability of $[\text{Cp}^*\text{Mo}_2\text{Br}_4]^+$, which is the reason for the redox stability of system B ($\text{X} = \text{Br}$) in solution and of the solid-state structure of $\{[\text{Cp}^*\text{Mo}_2\text{Br}_4]^+[\text{Cp}^*\text{MoBr}_4]^-)_2\cdot\text{Cp}^*\text{MoBr}_4$. It is remarkable that this electrochemically stable system contains molybdenum centers in three different oxidation states, albeit all having an identical coordination geometry.

The electrochemical studies (Figure 2) also rationalize the electrochemical stability of system C for both $\text{X} = \text{Br}$ and I . Both the X^- and the X_3^- ions are electrochemically stable within the region of stability of the corresponding mixed-valence cation. In our preliminary account of the $[\text{Cp}^*\text{Mo}_2\text{I}_4]^+\text{I}_3^-$ compound,¹³ we commented that the electrochemical behavior of this species suggested that a neutral $\text{Cp}^*\text{Mo}(\text{IV})$ –iodide would be unstable. This is because the Mo(IV) species $[\text{Cp}^*\text{Mo}_2\text{I}_4]^{2+}$ would have a sufficiently high oxidation potential to oxidize I^- ions to I_2 . At that time, we did not consider the ability of additional I^- donor ligands to buffer the oxidizing power of the dication, which is of course the reason for the stability of $\text{Cp}^*\text{Mo}_2\text{I}_6$ (purple Cp^*MoI_3). If one or more Mo–I bonds could dissociate from the metal, an internal redox process would then take place. This is probably the initial step of the isomerization of purple Cp^*MoI_3 (A) to green Cp^*MoI_3 (C), which is triggered by electrochemical oxidation, by diiodine oxidation, or by thermal treatment.

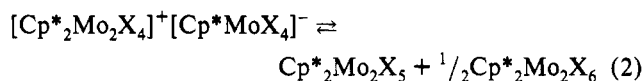
It is interesting to note that, from the electrochemical standpoint, the properties of the central metal ion are changed only to a limited extent by a change of halide. The $E_{1/2}$ for the $\text{Cp}^*\text{Mo}_2\text{X}_4/[\text{Cp}^*\text{Mo}_2\text{X}_4]^+$ and $[\text{Cp}^*\text{MoX}_4]^-/\text{Cp}^*\text{MoX}_4$ couples differ only by the rather small amount of ca. 20 mV on going from $\text{X} = \text{Cl}$ to $\text{X} = \text{Br}$, the more positive values being observed for the bromide system. This trend is analogous to the potential increase observed for the $[\text{CpVX}_3]^-/\text{CpVX}_3$ on going from Cl to Br system.¹⁰ On the other hand, the trend is reversed upon going further to the iodide system (Figure 2). These differences in potentials are, however, small and do not rationalize the vast difference in stability and reactivity observed for the “ Cp^*MoX_3 ” systems as X is changed from Cl to Br to I. Large differences in potentials are observed for the electrochemical processes of the free X^- ions. As a result of the easy oxidation of the I^- ligand, a neutral Cp^*MoI_4 species is nonexistent, and the highest possible oxidation state for a Cp^*Mo –iodide system is IV. This is one of the important reasons for the different behavior of different halide systems (e.g. the greater stability of form C with respect to form A when $\text{X} = \text{I}$ and the opposite when $\text{X} = \text{Br}$). The other determinant factor in this chemistry is the Lewis acidity of the $[\text{Cp}^*\text{Mo}_2\text{X}_4]^+$ cations, as will be discussed in the next section.

(b) Stability and Reactivity Trends and Mechanisms. We have seen above and provided a rationale for the fact that all three forms in scheme 3 exist for $\text{X} = \text{Br}$. However, forms B (obtained *in situ* by the redox reaction of $\text{Cp}^*\text{Mo}_2\text{Br}_4$ and Cp^*MoBr_4 in

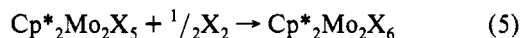
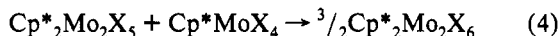
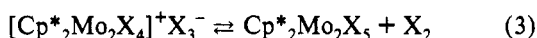
(34) Kubacek, P.; Hoffmann, R.; Havlas, Z. *Organometallics* 1982, 1, 180.

(35) Poli, R.; Owens, B. E.; Linck, R. G. *J. Am. Chem. Soc.* 1992, 114, 1302.

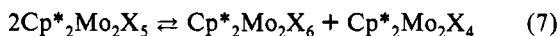
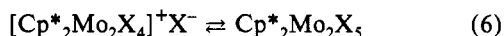
a 1:2 ratio) and **C** (obtained by decarbonylation of $\text{Cp}^*\text{MoBr}_3(\text{CO})_2$ in refluxing toluene or by oxidation of $\text{Cp}^*\text{Mo}_2\text{Br}_4$ with Br_2 , the latter having a nonequivalent amount of Br^- and Br_3^- ions) are reactive and redistribute in CH_2Cl_2 solution to an equilibrium mixture of **A** and **B**. We can conclude that the relative stability of the Br systems in CH_2Cl_2 solution is: $\text{C} < \text{A} \approx \text{B}$. For $\text{X} = \text{I}$, on the other hand, only forms **A** and **C** are found to exist, the latter being the thermodynamically more stable form ($\text{B} \ll \text{A} < \text{C}$). The nonexistence of **B** ($\text{X} = \text{I}$) is due to the nonexistence of the Mo(V) species Cp^*MoI_4 , as demonstrated by the electrochemical studies. Finally, only form **A** is stable for the chloride system (**B**, $\text{C} \ll \text{A}$).⁹ Forms **B** and **C** are predicted to be stable from the electrochemical standpoint (see Figure 2), but the reactions that would in principle lead to their formations ($\text{Cp}^*\text{Mo}_2\text{Cl}_4 + 2\text{Cp}^*\text{MoCl}_4$ for **B**; $\text{Cp}^*\text{Mo}_2\text{Cl}_4 + \text{PhICl}_2$ for **C**), lead to $\text{Cp}^*\text{Mo}_2\text{Cl}_6$ (form **A**) instead. This phenomenon can be ascribed to the high reactivity (Lewis acidity) of the $[\text{Cp}^*\text{Mo}_2\text{Cl}_4]^+$ ion. Even when $\text{Cp}^*\text{Mo}_2\text{Cl}_4$ and Cp^*MoCl_4 are allowed to react in a 1:1 ratio, the resulting $[\text{Cp}^*\text{Mo}_2\text{Cl}_4]^+ - [\text{Cp}^*\text{MoCl}_4]^-$ salt rapidly decomposes by chloride transfer to form the neutral $\text{Cp}^*\text{Mo}_2\text{Cl}_5$ and $\text{Cp}^*\text{Mo}_2\text{Cl}_6$ products (eq 2, $\text{X} = \text{Cl}$).⁹



The difference of reactivity between the chloro and bromo systems is remarkable. For the chloro system, reaction 2 is totally shifted toward the right,⁹ whereas for the bromo system it is totally shifted toward the left, e.g. the $[\text{Cp}^*\text{Mo}_2\text{Br}_4]^+[\text{Cp}^*\text{MoBr}_4]^-$ salt is perfectly stable *in the absence of additional Cp*MoBr₄*. Only when additional Mo(V) complex is present, a small equilibrium concentration of $\text{Cp}^*\text{Mo}_2\text{Br}_6$ is produced. We assume that the formation of $\text{Cp}^*\text{Mo}_2\text{Br}_6$ from the oxidation of $\text{Cp}^*\text{Mo}_2\text{Br}_4$ by Cp^*MoBr_4 or Br_2 proceeds mechanistically in the same way as observed for the corresponding chloride system, that is through the formation of the pentabromo species as a result of the halide transfer shown in eqs 2 and 3. This pentabromide species could then be oxidized by an excess of the oxidizing agent (eqs 4 and 5). Contrary to the chloro system, a pentabromo species does not accumulate in solution. This could be due to the slow rate of its formation by reactions 2 and 3 as compared by the rate of its consumption by reactions 4 and 5.



However, the situation appears to be further complicated. The reaction between $[\text{Cp}^*\text{Mo}_2\text{Br}_4]^+$ (BF_4^- salt) and Br^- was run with the intention to produce this pentabromide species in the absence of additional oxidizing agents (eq 6). Under these conditions, the slow formation of $[\text{Cp}^*\text{MoBr}_4]^-$ occurs but, once again, no evidence of the accumulation of a $\text{Cp}^*\text{Mo}_2\text{Br}_5$ species is obtained. We rationalize this observation by invoking the disproportionation of the pentabromo species in eq 7.



The hexabromo compound reacts immediately with the excess Br^- present in solution to afford the observed $[\text{Cp}^*\text{MoBr}_4]^-$ ion, whereas the tetrabromo compound engages in a fast self-exchange reaction with the corresponding paramagnetic cation with

consequent averaging of their $^1\text{H-NMR}$ signals. Reaction 6, like reaction 2, depends markedly on the nature of the halide ligands. The behavior of the bromo system just described should be compared with the rapid and quantitative reaction for $\text{X} = \text{Cl}$,⁹ and the total absence of a reaction for $\text{X} = \text{I}$ (green Cp^*MoI_3 does not react with I^-). This difference demonstrates the large variation in Lewis acidity of the $[\text{Cp}^*\text{Mo}_2\text{X}_4]^+$ ions in the order $\text{Cl} > \text{Br} > \text{I}$.

What could be the reason for this marked trend of Lewis acidity? The addition of X^- to this quadruply-bridged cation is likely to open up one bridge and afford a species of structure $\text{Cp}^*\text{XMo}(\mu-\text{X})_3\text{MoX}\text{Cp}^*$ with possible partial relief of steric strain. Thus, a difference in steric strain in the precursor as the nature of X is changed could in principle cause a difference in reactivity. However, a comparison of the structural parameters of the $[\text{Cp}^*\text{Mo}_2\text{X}_4]^+$ ($\text{X} = \text{Br}, \text{I}$) ions investigated in this study, in particular the angular parameters of the $\text{Mo}(\mu-\text{X})_3\text{Mo}$ core, does not show major differences. As the Mo-X distances increase on going from $\text{X} = \text{Br}$ to $\text{X} = \text{I}$, so does also the Mo-Mo distance and as a result the CNT-Mo-X and X-Mo-X angles do not vary significantly. A structure of the more reactive $[\text{Cp}^*\text{Mo}_2\text{Cl}_4]^+$ species has not been determined (in fact such species could not be isolated)⁹ but structures of similar *neutral* (ring)₂ Mo_2Cl_4 compounds^{21,19} have angular parameters similar to those of the tetrabromo- and tetraiodo-bridged cations reported here, and we have shown above that these parameters are not sensitive to the electronic configuration of the complex (d^2-d^3 vs d^3-d^3). The difference in reactivity of these ions can perhaps be rationalized on the basis of the known greater tendency of the heavier, softer and less electronegative halide ions to occupy bridging positions with respect to the lighter analogues. It is only remarkable that this difference can cause such a dramatic change of reactivity as observed here for the series of $[\text{Cp}^*\text{Mo}_2\text{X}_4]^+$ ions.

The halide transfer from the $\text{Cp}^*\text{MoX}_4^-$ anion to the $[\text{Cp}^*\text{Mo}_2\text{X}_4]^+$ cation in reaction 2 could in principle proceed through dissociation of X^- from the anion followed by incorporation into the cation, or an associative mechanism could operate with the formation of an intermediate neutral trimetallic species. Investigations of mixed-halide conproportionation reactions, reported separately,³⁶ rule out the dissociative mechanism and also provide additional useful information on this halide transfer reaction.

The mechanism of the reaction between "Cp* MoX_3 " species and neutral donors L to afford adducts (either 18-electron bis-adducts for $\text{L} = \text{CO}$ or 16-electron mono-adducts for $\text{L} = \text{PMe}_3$, X^-) is easily rationalized on the basis of the results of our experiments: the only reactive form is **A** which, being unsaturated, can be attacked by L, followed by splitting of the $\text{Mo}_2(\mu-\text{X})_2$ bridge. Splitting of such dimeric unit is rapid because there is no metal-metal bond to be broken. After this step, the 16-electron $\text{Cp}^*\text{MoX}_3\text{L}$ complex may then coordinate another L ligand if this is sufficiently small (e.g. CO) to fit in the coordination sphere. Forms **B** and **C** of "Cp* MoX_3 " do not react with L ligands directly, but they can react indirectly via preequilibration with the reactive form **A** (only for $\text{X} = \text{Br}$). Because of microscopic reversibility, the thermal decarbonylation of $\text{Cp}^*\text{MoX}_3(\text{CO})_2$ must afford **A** as the kinetically controlled product. This is verified experimentally for the iodide system, which affords **A** from refluxing CH_2Cl_2 and **C** under more forcing conditions. For the bromide system, pure samples of **A** have not been obtained by this method, because these establish the equilibrium with **B** relatively rapidly in refluxing CH_2Cl_2 .

Finally, the reactions of $[\text{Cp}^*\text{MoCl}_2]_2$ with HX are worth a brief discussion. The results of these reactions indicate that the proton in HX ($\text{X} = \text{Br}, \text{I}$) has sufficient oxidizing power to convert the $[\text{Cp}^*\text{MoX}_2]_2$ materials to the corresponding monocations, the other redox product of the reaction being presumably H_2 . It has been however reported that treatment of $[(\eta\text{-C}_5\text{H}_4\text{R})_2\text{Mo}_2$

Cl_5^- ($\text{R} = \text{Me}, i\text{-Pr}$) (a product of the reaction between $[(\eta\text{-C}_5\text{H}_4\text{R})\text{MoCl}_2]_2$ and Cl^-) with HCl regenerates the neutral dinuclear Mo(III) compound.³⁷ In agreement with this report, we find no reaction between $[\text{Cp}^*\text{MoCl}_2]_2$ and HCl in CH_2Cl_2 . Since the change of halogen has a negligible effect on the redox potential for the $\text{Cp}^*_2\text{Mo}_2\text{X}_4/\text{Cp}^*_2\text{Mo}_2\text{X}_4^+$ couple, the most likely reason for the difference observed in the $[\text{Cp}^*\text{MoCl}_2]_2/\text{HX}$ reaction when X changes from Br or I to Cl is the reduced oxidizing power of the HCl proton with respect to the protons of HBr and HI in organic solvents, which may be correlated with the greater strength of the HCl bond.

Conclusions

In summary, we have established a number of things with the present study and the parallel study of the corresponding chloride system.⁹ Cyclopentadienylmolybdenum(IV) trihalide compounds exist in different forms (see Scheme 3), the most stable of which depends on the nature of the halide. Very rarely is such a variety of structural types and such a dramatic change of relative stability observed by merely changing the nature of the halogen atoms. The thermodynamically more stable forms are as follows: A for $\text{X} = \text{Cl}$; B for $\text{X} = \text{Br}$; C for $\text{X} = \text{I}$. These findings show that the extrapolation of the chemistry of one halide system to another is an exercise that should be done with caution.

The influence of the halide is reflected mainly in two different variables: the oxidation potential of the X^- ion and the Lewis acidity of the $[\text{Cp}^*\text{Mo}_2\text{X}_4]^+$ complex. Thus, for instance, the ionic structure C containing the reduced $[\text{Cp}^*\text{Mo}_2\text{X}_4]^+$ ion and the oxidized X_3^- ion is favored with respect to the neutral Mo(IV) structure A, $\text{Cp}^*\text{Mo}_2\text{X}_6$, when $\text{X} = \text{I}$ but disfavored when $\text{X} = \text{Br}$. Also, whereas $[\text{Cp}^*\text{Mo}_2\text{Cl}_4]^+$ scavenges Cl^- from the $\text{Cp}^*\text{MoCl}_4^-$ ion,⁹ the $[\text{Cp}^*\text{Mo}_2\text{Br}_4]^+[\text{Cp}^*\text{MoBr}_4]^-$ salt is stable in the absence of oxidizing equivalents (e.g. Cp^*MoBr_4 or Br_2) but the cation reacts *slowly* with free Br^- , and finally the $[\text{Cp}^*\text{Mo}_2\text{I}_4]^+$ does not react with free I^- . Parallel mixed-halide studies, which have been reported separately,³⁶ confirm the conclusions reached here concerning the Lewis acidity of $[\text{Cp}^*\text{Mo}_2\text{X}_4]^+$: $[\text{Cp}^*\text{Mo}_2\text{Cl}_4]^+$ rapidly scavenges a halide from either $[\text{Cp}^*\text{MoCl}_4]^-$ or $[\text{Cp}^*\text{MoBr}_4]^-$, whereas $[\text{Cp}^*\text{Mo}_2\text{Br}_4]^+$ does not scavenge a halide from either anion.

(37) Feng, Q.; Ferrer, M.; Green, M. L. H.; Mountford, P.; Mtetwa, V. S. *B. J. Chem. Soc., Dalton Trans.* 1992, 1205.

The only reactive form of “ Cp^*MoX_3 ” with respect to ligand addition reactions is $\text{Cp}^*\text{Mo}_2\text{X}_6$. The other forms (e.g. B and C) can only add neutral ligands if they first equilibrate with A, which is possible for the Br system but not for the I system. Electrochemically, there is little difference between the $[\text{Cp}^*\text{Mo}_2\text{X}_4]^{0/+2+}$ and $[\text{Cp}^*\text{MoX}_4]^{0/-}$ systems with different X ligands, but the low oxidation potential of I^- to I_3^- makes Cp^*MoI_4 a nonexistent compound.

All structures determined for Cp^*Mo halide systems in the oxidation states from III to V exhibit the ubiquitous four-legged piano stool geometry around each metal center, the proper X/Mo stoichiometry being maintained by sharing a different number of bridging halides in dinuclear structures. The interplay between oxidation potential and the buffering of this by X^- coordination is responsible for the existence and stability of system B ($\text{X} = \text{Br}$) in solution and of $\{[\text{Cp}^*\text{Mo}_2\text{Br}_4]^+[\text{Cp}^*\text{MoBr}_4]^-_2\}\text{Cp}^*\text{MoBr}_4$ in the solid state. These systems contain molybdenum atoms in three different oxidation states, although all of them have the same coordination environment (four-legged piano stool Cp^*MoBr_4). Structurally, we find that the d^2-d^2 $\text{Cp}^*\text{Mo}_2\text{X}_6$ ($\text{X} = \text{Br}, \text{I}$) compounds are identical to the corresponding chloro analogue⁹ (e.g. nonbonded structure I) and to the d^1-d^1 Ta(IV) dimers,²⁵ whereas they are different than the d^3-d^3 Re(IV) dimers,²⁶ the latter adopting the metal–metal-bonded structure II. On topic of current interest in our laboratory is to establish whether the yet unknown W(IV) analogues would prefer structure II, given the fact the W is known to establish stronger metal–metal bonds with respect to molybdenum.

Acknowledgment. We are grateful to the DOE-OER for support of this work. We also thank Prof. G. Parkin for informing us of the method of preparation of $[\text{Cp}^*\text{MoI}_2]_2$ discovered in his laboratory and for a preprint of ref 16b.

Supplementary Material Available: Full tables of crystal and refinement parameters, bond distances, bond angles, anisotropic thermal parameters, and hydrogen atom positions for compounds $\text{Cp}^*\text{Mo}_2\text{Br}_6$ ($C2/c$), $\text{Cp}^*\text{Mo}_2\text{Br}_6$ ($P2_1/n$), $\text{Cp}^*\text{Mo}_2\text{Br}_6\text{C}_6\text{H}_6$, $\text{Cp}^*\text{Mo}_2\text{Br}_4$, $\{[\text{Cp}^*\text{Mo}_2\text{Br}_4]^-[\text{Cp}^*\text{MoBr}_4]^+\}_2\text{Cp}^*\text{MoBr}_4\cdot 2\text{C}_7\text{H}_{16}$, $[\text{Cp}^*\text{Mo}_2\text{I}_4]\text{I}_3$, $[\text{Cp}^*\text{Mo}_2\text{Cl}_x\text{I}_{4-x}]_3$ and $[\text{NMe}_3\text{Ph}][\text{Cp}^*\text{MoI}_4]$ (55 pages). Ordering information is given on any current masthead page.